國 立 交 通 大 學

環 境 工 程 研 究 所

博 士 論 文

全域最佳解應用於地下水抽水源鑑定分析

Applications of Global Optimization Method for

Solving Groundwater Pumping Source

Identification Problems

研 究 生：林 郁 仲

指導教授：葉 弘 德 教授

中 華 民 國 九 十 五 年 八 月

全域最佳解應用於地下水抽水源鑑定分析

Applications of Global Optimization Method for Solving Groundwater
Pumping Source Identification Problems

研 究 生：林郁仲 　　　　　Student : Yu-Chung Lin

指導教授：葉弘德 　　　　　Advisor : Hund-Der Yeh

國 立 交 通 大 學

環境工程研究所

博士論文

A Dissertation

Submitted to Institute of Environmental Engineering

College of Engineering

National Chiao Tung University

for the Degree of

Doctor of Philosophy

in Environmental Engineering

August 2006

Hsinchu, Taiwan

中 華 民 國 九 十 五 年 八 月

全域最佳解應用於地下水抽水源鑑定分析

研究生：林郁仲　　　　指導教授：葉弘德

國立交通大學環境工程研究所

中文摘要

地下水為一珍貴的天然資源因此私人開發受法律條文限制，不可違法取用。當某一地下水發現遭受擅自取用，藉由觀測的地下水位來推求抽水源位置、抽水量、及抽取時間，則為需要探知的問題。因此本研究發展一個方法，藉由模擬退火演算法的優點，結合美國地質調查局所研發之三維地下水流模擬模式MODFLOW-2000，做為抽水源鑑定的工具，針對在監測井所量測得的地下水水位，推求地下水抽水源的位置、抽水量、及抽取時間。為驗證所發展方法的正確性，先假設某一抽水源抽取地下水，藉用 MODFLOW-2000 模式模擬該地下水系統的水力水頭分布。

隨後在利用所發展的方法，進行抽水源鑑求。首先選擇一個區域，設為可疑的抽水源區域。其次以模擬退火演算法，在可疑抽水源區域選定抽水源位置，

並產生該抽水量及抽取時間的試誤解。最後再以 MODFLOW-2000 進行相關的水力模擬，以得到在各監測井的模擬地下水水位。當所得結果滿足所設定的目標函數時，亦即模擬水位高與實際水位高差值的平方和最小時，即表示求得正確的抽水源位置、抽水量、及抽取時間。由數值模擬的結果顯示，即便在均質含水層、非均質含水層、或是其觀測水位包含誤差，本研究所發展的方法，依然能得到精確的推估結果。

關鍵字：地下水、MODFLOW、抽水源鑑定、最佳化、模擬退火演算法

Applications of Global Optimization method for Solving Groundwater
Pumping Source Identification Problems

Student : Yu-Chung Lin   Advisor : Hund-Der Yeh

Institute of Environmental Engineering

National Chiao Tung University

ABSTRACT

Groundwater is a precious water resource on earth.   In the real world, if the groundwater is illegally pumped, the information including pumping source location, pumping rate, and pumping period are the important information and needed to be identified.   Locating the unknown source is an inverse problem and can be considered as a pumping source identification problem.   An approach, using the simulated annealing and a three-dimensional groundwater flow model (MODFLOW-2000) is developed to estimate the pumping source information.   In order to verify the validity of the present approach, a pumping well is assumed to install at known location and withdraws the groundwater at a known pumping rate.

After a specified time, the hydraulic head (hereafter called observed head) at

observation wells can be simulated by MODFLOW.   Then the proposed approach is

chosen to estimate the pumping source information when minimizing the sum of

square errors between the simulated heads and observed heads at the observed wells.

In the estimation process, a series of trial solutions for source location, pumping rate,

and pumping period are generated by simulated annealing (SA).   Then the

MODFLOW-2000 is employed with those generated source information to simulate

the hydraulic distribution at observation wells.   Those procedures are repeatedly

until the sum of square error between simulated head and measured head is minimized.

The proposed approach gives good estimated results in both synthetic and real

problems even the measured heads contain measurement errors.

KEYWORDS: Groundwater,   MODFLOW,   pumping   source   identification,

optimization, simulated annealing

致謝

甫自 2000 年迄今，於交大環工所，也已渡過了六個年頭。在這六年間，非常由衷感謝我的指導教授葉弘德老師，若沒有老師嚴謹細心的指導與教誨，今天我也無法如此順遂的完成博士學業。

在這六年間，從老師身上學習到最大的資產，即為老師嚴謹的治學精神，及其持之以恆的學習心態。猶記當年，因蝴蝶曼妙的姿態，展開了老師另一個生活的樂趣。為了徹底瞭解蝴蝶的種類，老師一覽圖書館中，所有蝴蝶的藏書。為了更深入瞭解蝴蝶的棲息生態，老師發揮了「愛屋及烏」的胸襟，認真研究所有的花草。現在老師的生活中，除了古典音樂及石頭外，另外「擴充」了蝴蝶與花草的經驗與知識，更讓老師的平日生活，增色不少。老師除了在地下水的專業知識外，亦能再另一個陌生的領域中，發光發熱。我想，這就是在這六年來，老師帶給我最大的感動，更讓我瞭解到，學海無涯的精神。

其次仍要感謝口試委員：葉高次教授、童慶斌教授、陳主惠教授、劉振宇教授、及蔡惠峰博士，對本論文的不吝指正及建議，使得本論文得以更為完整。

再來亦需感謝地下水實驗室的伙伴，感謝智澤學長、彥禎、雅琪、彥如、及嘉真等同修間的相互砥礪與扶持，使得所有的研究論文，得以順遂完成；感謝桐樺、淇汾、易璁、敏筠、毓婷、士賓、及博傑等學弟妹的協助，讓所有進行的研究工作，得以平順進行；感謝廷光、長祺、智雄、及盛欽的陪伴，讓我在這段

生活中，增添許多歡笑與色彩。

　　最後，仍由衷感謝家人們的支持與鼓勵，感謝父親、岳父、及岳母，在這段時間的鼓舞與關心；感謝瑞芬在這段「取經」的旅程中，無悔的付出與支持。最後僅將此論文，獻給我愛的家人：瑞芬、韋翰、韋伶、及所有支持我的家人。

　　猶記口試完當天，在開車回台北的路上，一面聆聽貝多芬的「命運」交響曲，一面回首咀嚼過往的成長。在成長的道路上，有歡笑，也有淚水，但只要堅持下去，相信最後成功的果實，一定會是甜美的，也如同那「命運」交響曲中的第四樂章，澎湃激昂。

<div align="right">

郁仲　謹致於

國立交通大學環境工程研究所

2006 年 8 月

</div>

TABLE OF CONTENTS

LIST OF TABLES

LIST OF FIGURES

NOTATION

E	：	System energy
Er	：	The level of measurement error
$f(x)$	：	Objective function value of x
$f(x')$	：	Objective function value of x'
h	：	Hydraulic head
$h_{ij.mes}$	：	Measured head measured at jth time step in ith observation well
$h_{ij,sim}$	：	Simulated head measured at jth time step in ith observation well
K_{ij}	：	Hydraulic conductivity
k	：	Boltzman's constant
lnK	：	Logarithm hydraulic conductivity
λ	：	Correlation length
N	：	Number of considered variables
nm	：	Number of observation wells
NS	：	Number of cycles
$nstep$	：	Number of the time step
NT	：	Number of iterations before temperature reduction
$P(E)$	：	Occurrence probability
P_{SA}	：	Acceptance probability of the trial solution x'
RD	：	Random number
R_{Te}	：	Temperature reduction factor
S_s	：	Specific storage
σ_y	：	Standard deviation of the natural logarithm of hydraulic conductivity
t	：	Time

Te	：	Temperature
VM	：	The step length vector
W	：	Volumetric flux per unit volume
x	：	Trial solution
x'	：	The neighborhood trial solution
x_i	：	The Cartesian coordinates
$\bar{y}$	：	The mean of the natural logarithm of hydraulic conductivity

CHAPTER 1 Introduction

1.1 Background

The amount of water on earth is estimated about 1,386 million cubic kilometers (km^3), with about 2.5 % of it is potable freshwater. However, about 68.7 % of freshwater is unavailable due to the water is tied up in glaciers. In addition, 30.1 % of freshwater is found in subsurface and 0.2 % of freshwater is the surface water. Obviously, the quantity of the groundwater is reliable for human usage. Concerning the quantity, few suspended solids, small concentrations of bacteria and virus, and only minimal concentrations of dissolved mineral salts are the important characteristics to make the natural groundwater an ideal freshwater resource to support human life [*Todd and Mays*, 2005]. Therefore, the groundwater resource reveals its precious significance as the surface freshwater is shortage for domestic or industrial usage.

The effective and appropriate management strategy to the groundwater usage can provide the fresh groundwater for human uses and environmental functions. Comparatively, if the groundwater is abused, adverse effects occur. These adverse effects include seawater intrusion into coastal aquifer, land subsidence, aquifer dewatering and increased pumping costs, upwelling of low-quality groundwater into

freshwater aquifer [*Loáiciga*, 2004].

To avoid the negative occurring, the numerical simulation model, built from the flow and transport equation, is usually employed to predict the response of the system for different excitation. As a result, the manger or engineer can use the simulation model to solve or analyze the management problem. *Bear* [1979] indicated that the management problem could be solved by incorporating a simulation model with an optimization program. Therefore, the different management decisions are compared and an optimal decision is selected based on certain criteria.

Optimization problem is an inherent intractable problem. Traditionally, linear programming, nonlinear programming, or Newton-type approach is often employed to solve the optimization problem. The gradient-type approaches are difficult in finding optimal solutions for large–scale combinatorial optimization problems and parameter estimation problems with complex search spaces [*Cai et al.*, 2001]. In general, two difficulties might perplex the inexperienced users. Depending on the starting point in the search process, the gradient-type approaches may give a local optimal result. *Cai et al.* [2001] pointed out that if an improper initial guess is given, the gradient-type approaches generally converge to a local solution nearest to the starting point. Therefore, the first problem of using gradient-type approaches is to give an improper initial guess. In addition, the gradient-type approaches need to

compute the derivatives with respect to decision variables to iteratively update the solution for obtaining the optimal solution. The second problem is that those derivatives may be difficult to calculate analytically or numerically in highly nonlinear and nonconvex optimization problems [*Shieh and Peralta*, 2005].

Stochastic optimization methods such as genetic algorithms (GAs) and simulated annealing (SA) are the new global optimization solvers. Differed from the gradient-type approaches, these global optimization methods are iteratively to renew the trial solution by the objective function value for determining the nearby global optimum. The first advantage of these global optimization methods is that the user does not need much experience in providing the initial guesses for solving non-linear problems. The initial guesses can be arbitrary given or even generated by a random number generator, and can still achieve optimal results. The second advantage is that these global optimization methods do not need to calculate the analytical or numerical derivates to renew the trial solution.

SA is a random search algorithm that allows, at least in theory or in probability, to obtain the global optimum of a function in any given domain. The philosophy of SA is to imitate the physical annealing process that heating up a solid and then cooling it down slowly until it crystallizes. As the temperature is reduced properly, a regular crystal structure is obtained and its enthalpy is minimal. If the cooling

process is carried too fast, an irregularities structure is obtained and the system does

not reach the minimum enthalpy state.

Similar to Newton's type methods, SA starts with a single initial guess. The

initial guess is used to calculate the objective function value and then renamed as the

current optimum. A series of trial solutions are generated from the current optimal

solution within the boundary to renew the optimal solution on the basis of the

objective function value obtained from the trial solution. To avoid obtaining local

optimum, the Metropolis mechanism controls which ascent moves could be accepted

[*Rayward-Smith et al.*, 1996]. The algorithm will be terminated when SA obtains the

optimal solution or the obtained solution satisfies the stopping criteria.

1.2 Objectives

The groundwater resource usually is not allowed to pump for private usage

without permit. Illegal pumping may have an adverse effect on the groundwater

flow system and impair the quantity and quality of the groundwater of a remediation

site. Such an illegal pumping may change the groundwater flow pattern and disturb

the capture zone delineation at an ongoing remediation site. Thus, there is a need to

develop a methodology for estimating the unknown pumping source location and

pumping rate from a practical viewpoint.

The main objective is to develop an approach using SA incorporated with the

numerical flow model, modular three-dimensional finite-difference ground-water flow

model (or called MODFLOW-2000), to estimate the pumping source location,

pumping rate, and pumping period in a groundwater flow system. A hypothetic

pumping well is assumed at a specific location and withdraws the groundwater with a

specified flow rate. The water level (hereafter called measured head) at the

observation wells can be simulated by the MODFLOW-2000. Then the developed

approached is launched to determine the pumping source location, pumping rate, and

pumping period with the measured head at observation wells.

In the pumping source information estimation process, SA is responsible for

generating a series of trial solutions for the pumping source location, pumping rate,

and pumping period. These trial solutions are then used as input in

MODFLOW-2000 to calculate the simulated heads. The pumping source location,

pumping rate, and pumping period can be determined by the proposed approach when

minimizing the sum of square errors between the simulated heads and measured heads

at the observation wells.

CHAPTER 2 Literature Reviews

SA is a stochastic computational technique derived from statistical mechanics for finding nearby-global optimal solution to large optimization problems. *Metropolis et al.* [1953], the first forerunner, applied SA to a two-dimensional rigid-sphere system. *Kirkpatrick et al.* [1983] employed it in solving large-scale combinatorial optimization problems. SA is an evolution from descent search method, but the major drawback of the descent method was the obtained solution might end up in a local optimum [*Rayward-Smith et al.*, 1996]. The significant difference between SA and descent method is that the SA used Metropolis mechanism, or called the Boltzman's mechanism, to control which ascent moves could be accepted. Therefore, the SA has a property of using descent strategy but allowing random ascent moves to avoid possible trap in a local optimum, preventing the SA from having the same problem as the descent method.

SA was successfully applied in wide range of optimization applications such as capacity extension for pipe network system [*Cunha and Sousa*, 1999; *Monem and Namdarian*, 2005], parameter calibration and identification problems [*Zheng and Wang*, 1996; *Cooper et al.*, 1997; *Li et al.*, 1999; *Guo and Zheng*, 2005; *Lin and Yeh*, 2005; *Yeh et al.,* 2005], groundwater management problems [*Dougherty and Marryott*, 1991; *Marryott et al.*, 1993], groundwater remediation system problems [*Kuo et al.*,

1992; *Marryott*, 1996; *Rizzo and Daugherty*, 1996; *Shieh and Peralta*, 2005], and source identification of groundwater contamination problems.

Romeo and Sangiovanni-Vincentelli [1991] used homogeneous and inhomogeneous Markov chain theories to prove that SA can converge to global optimal solutions. *Goffe et al.* [1994] employed SA to solve four econometric problems and compare the results obtained from the convectional algorithms. Their solutions obtained from SA indicated those were global optimum and superior to the solutions obtained from the convectional algorithms. Their results also indicated that SA is a very robust algorithm. *Habib et al.* [2001] applied evolutionary algorithms, SA and tabu search, on the same optimization problem and compared with the quality of the best solution identified by each heuristic, the progress of the search from initial solutions until stopping criteria are met, the progress of the cost of the best solution as a function of time, and the number of solutions found at successive intervals of the cost function.

Cunha and Sousa [1999] used SA to minimize the capacity extension cost in the water distribution network. Their results obtained from SA and nonlinear programming (NLP) techniques for several medium size networks showed that SA did provide a better solution in general, in comparison with that obtained from the NLP technique. *Shieh and Peralta* [2005] used the hybrid genetic algorithm-simulated

annealing to optimize in situ bioremediation system design. They mentioned that the straightforward formulation, no requirement for computing derivatives, and easily implemented with ground water simulation models, are the main advantages of SA to solve the optimization problem.

For the parameter calibration and identification problems, *Zheng and Wang* [1996] treated the problem of identifying optimal parameter structure as a large combinatorial optimization problem. In groundwater modeling, the identification of an optimal flow or transport parameter that varies spatially should include both the values and structure of the parameter. They employed the tabu search and SA to solve the combinatorial optimization problem. Their result indicated that the proposed approaches perform extremely well when compared with those obtained from the grid search or descent search. *Tung et al.* [2003] developed an optimal procedure for applying SA and the short distance method with MODFLOW to determine the best zonation of hydraulic conductivity by minimizing the errors of hydraulic head. Their results illustrated that the procedure can effectively determine and delineate the hydrogeological zone. *Yeh et al.* [2005] proposed a novel approach based on a groundwater flow model and SA to determine the best-fit aquifer parameters for leaky aquifer systems. The aquifer parameters obtained from SA almost agree with those obtained from the extended Kalman filter and gradient-type

method.   Moreover, all results indicated that the SA is robust and yielded consistent results when dealing with the parameter identification problems.

Recently, groundwater contamination problems have attracted much attention. When a groundwater site is detected to be contaminated, the investigators have to identify the potential responsible parties at the site and assist the responsible parties to do the clean work.   The source identification of groundwater contamination contains the determination for the source location or the source release history based on the measured contaminant concentrations at the sampling points.   *Atmadja and Bagtzoglou* [2001] reviewed the methods that had been developed during the past 15 years in identifying the source location and release history.   They classified the contaminant transport inversion methods into four different approaches, optimization approaches, probabilistic and geostatistical simulation approaches, analytical solution and regression approaches, and direct approaches.

Optimization approaches run forward simulations first and then use an optimization method to obtain the best-fit solution.   Probabilistic and geostatistical simulation approaches employ probabilistic techniques to identify the probability of the location of the sources.   Analytical solution and regression approaches provide a complete estimate of parameters of the pollutant.   Based on the deterministic methods, the direct approaches solve the governing equations reversely and

reconstruct the release history of the contaminant concentration plumes. As employed optimization approach to solve the inverse problem, the gradient-type or non-gradient-type approach with an iterative scheme is commonly employed to find the solution of nonlinear least-square equations obtained after taking the derivatives of the objective function with respect to the unknown parameters.

Atmadja and Bagtzoglou [2001] also divided the groundwater contaminant source identification problem into two categories. The first category is to determine the source location with a constant release concentration and period by the measured concentrations [e.g., *Hwang and Koerner*, 1983; *Bagtzoglou et al.*, 1992; *Mahar and Datta*, 1997, 2000, 2001]. *Hwang and Koerner* (1983) employed a modified finite element model with limited monitoring well data to minimize the sum of the square errors of the measured concentration and estimated concentration to identify the pollution source. *National Research Council* [1990] suggested using a trial-and-error method incorporated with a forward model to solve the problem of source information estimation. Bagtzoglou et al. (1992) proposed an approach using particle methods to provide probabilistic estimates of source location and time history in a heterogeneous site. Their study indicated that the simulation with conditional conductivity field performs as well as the simulation with perfectly known conductivity field. *Sciortino et al.* [2000] developed an inverse procedure based on

the Levenberg-Marquardt method and three-dimensional analytical model to solve the least squares minimization problem for identifying the source location and the geometry of a DNAPL pool. Their study showed that the result is highly sensitive to the hydrodynamic dispersion coefficient.

The second category is to use the measured concentrations for recovering the release history at a known source location. For identifying the release history problems, *Liu and Ball* [1999] further classified these problems into following two types: function fitting problem and full-estimation problem. Function fitting problem initially assumes the release history as a particular function and reformulates it as an optimization problem. A gradient-type approach or non-gradient-type approach is employed to estimate the best-fit parameters of the release function [*Gorelick et al.*, 1983; *Wagner*, 1992]. The full-estimation approach [e.g., *Skagg and Kabala*, 1994 1995, 1998; *Samarskaia*, 1995; *Woodbury and Ulrych*, 1996; *Snodgrass and Kitanidis* 1997; *Woodbury et al.*, 1998; *Liu and Ball*, 1999; *Neupauer and Wilson*, 1999, 2001; *Neupauer et al.*, 2000] is to reconstruct the release history by matching the estimated concentrations with the measured concentrations.

Additionally, the stochastic optimization methods are used to incorporate with the simulation models to solve the groundwater contaminant estimation problems. *Aral and Gaun* [1996] proposed an approach called improved genetic algorithm (IGA)

to determine the contaminant source location, leak rate, and release period. The results obtained from the IGA agreed with those obtained from linear and nonlinear programming approaches. *Aral et al.* [2001] proposed a new approach, named the progressive genetic algorithm (PGA) in which the GA is incorporated with the groundwater simulation model, for source identification problem. Their results indicated that the initial guess doesn't influence the identified solution. *Mahinthakumar and Sayeed* [2005] developed hybrid genetic algorithm-local search (GA-LS) methods to solve the groundwater source identification problem. GA was used to perform an initial search of decision space to obtain possible optimal solutions as the starting guesses. Then the local search was used to obtain the optimal solutions by fine-tuning these starting guesses. The algorithms they developed were applied to a two-dimensional homogeneous flow field with a total of 150 observation concentrations from 3 monitoring wells and a three-dimensional heterogeneous flow field with a total of 1800 observation concentrations from 18 monitoring wells. Their results indicated that the GA-LS were more effective for the groundwater source identification problems than individual approaches such as real encoded GA, conjugate gradient trust region method, Levenberg–Marquadt , Nelder–Meade simplex method, and Hooke-Jeeves method. *Sayeed and Mahinthakumar* [2005] used parallel implementation skill to demonstrate the performance of GA-LS and the
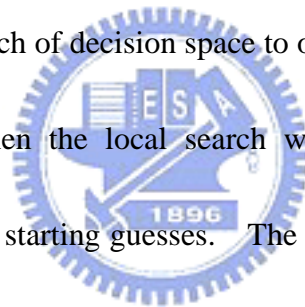
parallel groundwater transport and remediation codes (PGREM3D) in determining the

source location and recover the release history. They used a total of 1,800

observations from 18 observation wells to investigate single- and three-source

problems. *Mahinthakumar and Sayeed* [2006] further used GA-LS and PGREM3D

to recover the release histories for identifying the responsible parties. Four hybrid

algorithms, four local search methods, and the individual GA were used to test the

performance on recovering the release history problems in three-dimensional

heterogeneous conductivity fields. Their results indicated that the hybrid

optimization methods are very effective in solving these problems.

CHAPTER 3   Methodology

3.1 Groundwater Flow Model

The three-dimensional equation describing the groundwater flow can be expressed as [*Harbaugh and McDonald*, 1988]

$$\frac{\partial}{\partial x_i}\left(K_{ij}\ \frac{\partial h}{\partial x_i} \right) + W\ =\ S_s\ \frac{\partial h}{\partial t} \tag{1}$$

where h is the hydraulic head [L], K_{ij} is the hydraulic conductivity tensor [L/T], S_s is the specific storage [L^{-1}], W is the volumetric flux per unit volume representing sources and/or sink (negative for flow out and positive for flow in [L/T]), x_i are the Cartesian coordinates, and t is time [T].

Equation (1), together with specification of flow and/or head conditions at boundaries of an aquifer system and specification of initial head conditions, constitutes a mathematical model of a groundwater system.   A numerical approach to approximate the mathematical model can be employed to simulate the head distribution for a given aquifer system.   The computer model, an enhanced version of ground-water flow model, MODFLOW-2000 developed by the United State Geology Survey (USGS), is used to simulate the groundwater flow system.   The numerical model MODFLOW-2000 expends upon the modularization approach that was originally included in MODFLOW and simulates steady-state and transient flow

in an irregularly shaped flow system with the aquifer being confined, unconfined, or a

combination of confined and unconfined [*Harbaugh et al.*, 2000].

Packages, procedures, and modules are the essential modularization entities in all

the earlier versions of MODFLOW. The user can select a series of packages or

modules during a given simulation. The package, for the user's perspective, is

designed to divide the program into pieces and help user to simulate the different

kinds of groundwater flow problems. Individual packages may or may not be

required, depending on the problem being solved. The procedure, for the

programmer perspective, is designed to break the program into pieces that make the

program logic as simple as possible for programmer to maintain the desired

functionality. The modules can be grouped into packages or procedures that deal

with a single aspect of the simulation.
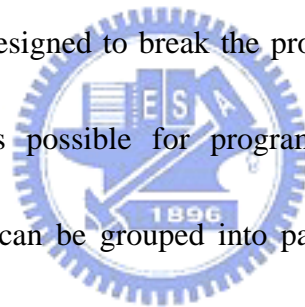
The major difference between MODFLOW-2000 and its earlier versions is that

the MODFLOW-2000 adds a new modularization entity called process to incorporate

the solution of multiple related equations. A process is a part of the code that solves

fundamental equation by a specified numerical method. For example, the

Ground-Water Flow process includes all aspects of solving the flow equation,

including the formulation of the finite-difference equations, data input, solving the

resulting simultaneous equations, and output. If a different method, the

finite-element method for example, is used, then this would become a separate process.   The processes, packages, and additional capabilities of MODFLOW-2000 are listed and briefly described in Table 1 [*Todd and Mays*, 2005].

3.2 Simulated Annealing

The concept of SA is based on an analogy to the physical annealing process.   At the beginning of the process, the temperature is increased to enhance molecule mobility.   Then, the temperature is slowly decreased to allow the molecules to form crystalline structures.   When the temperature is high, the molecules have high activity and have more freedom to arrange the configuration.   If the temperature is cooled properly, the crystalline configuration is the most stable state; thus, the minimum energy level may be reached naturally.

SA was modified from the descent method.   *Rayward-Smith et al.* [1996] mentioned that the drawback of the descent method was the obtained solution might end up in a local optimum.   In the SA, the Metropolis mechanism, or called the Boltzman's mechanism, is employed to control which ascent moves could be accepted. Such a mechanism has a property of using descent strategy but allowing random ascent moves to avoid possible trap in a local optimum, preventing the SA from having the same problem as the descent method.

As an iterative improvement method, an initial point *x* is required to evaluate the

objective function value $f(x)$.　Let x' be the neighbor of x and its objective function

value is $f(x')$.　The x' is given as

$$x' = x + (2 * RD_1 - 1) \times VM \qquad\qquad\qquad (2)$$

where RD_1 is a random number between zero and one from a uniform distribution and

VM is the step length vector.　In this study, the VM is automatically adjusted so that

approximately half of all evaluations are accepted.　In minimization problems, if $f(x')$

is smaller than $f(x)$, then the current optimal solution is placed with trial solution x'.

If $f(x')$ is not smaller than $f(x)$, then one has to test Metropolis's criteria and generate

another random number RD_2 between zero and one from a uniform distribution.　For

solving the minimization problem, the Metropolis's criterion is given as [*Pham and

Karaboga*, 2000]:
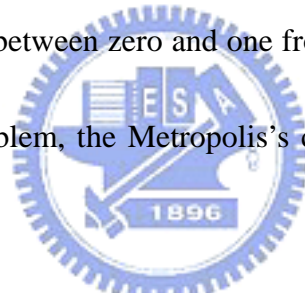
$$P_{SA} = \begin{cases} 1 & ,if \quad f(x') \le f(x) \\ \exp(\dfrac{f(x) - f(x')}{Te}) & ,if \quad f(x') > f(x) \end{cases} \qquad (3)$$

where P_{SA} is the acceptance probability of the trial solution and Te, a control

parameter, is usually the current temperature.　If the random number RD_2 is smaller

than P_{SA}, then the current solution also is placed with trial solution.　Otherwise, one

must continue generating the trial solution within the neighboring vicinity of the

current solution.　There exists a small probability that the system might have a high

energy even at a low temperature.　Note that, the acceptance probability P_{SA}

converges to one at high temperature as expressed in equation (3).　It also can be

found that there exists a small probability that the current optimal solution is replaced

with the ill solution.   This is the major reason why the solutions obtained from SA

may not be trapped in the local optimum or obtain an ill solution.

Figure 1 illustrates the algorithm of SA [*Pham and Karaboga*, 2000].   The first

step is to initialize the initial solution and set the initial solution to be the current

optimal solution.   Note that the number of considered variables is given as *N*.   The

second step is to update the current optimal solution, if the trial solution generated

from the initial solution within the boundary is better than the current optimal solution

or if the trial solution satisfies Metropolis's criterion; otherwise, continue generating

the trial solution.

After *NS* steps through all considered variables, the step length vector *VM* is

adjusted so that 50 % of all moves are accepted.   In other words, after *N*×*NS*

function evaluations, each element of *VM* is adjusted to the effect that half of all

function evaluations are accepted.   Note that the number of considered variables is

given as *N*.   The goal here is to sample the function widely.   If a general percentage

of points are accepted for *x'*, then the relevant of *VM* is enlarged.   For a given

temperature, this increases the number of rejections and decreases the percentage of

acceptances.   After *NT* times through the above loop, the temperature, *Te*, is reduced.

Accordingly, after *N*×*NT*×*NS* function evaluations, the temperature is decreased by

the temperature reduction factor R_{Te}.   Then the new temperature is given by

$$Te' = R_{Te} \times Te \qquad\qquad (4)$$

The value of R_{Te} is a constant smaller than one.   Typical value of R_{Te} is given as 0.85

[*Corana et al.,* 1987].   The temperature should be cooled properly to guarantee the

obtained solution is indeed the global optimal solution [*Zheng and Wang*, 1996].

The algorithm will be terminated when SA obtains the optimal solution or the

obtained solution satisfies the stopping criteria.   In general, the stopping criteria are

defined to check whether the temperature or the difference between the optimal

objective function value and those obtained in current iteration reach the specified

value or not.

3.3 Identification processes

This section illustrates how SA is incorporated with the groundwater flow model

to solve the pumping source identification problem.   This approach, called SA-MF,

combines SA and MODFLOW-2000 to solve the pumping source identification

problem.   Figure 2 demonstrates the flowchart of SA-MF which includes ten steps.

The first step is to initialize the initial solution.   All initial guess are generated by

random number generator within the solution domain.   The solution domains for

each unknown variable must be specified to confine the generated solution is

reasonable.   The   second   step   is   to   calculate   the   simulated   heads   by

MODFLOW-2000 with the guess values and the objective function value (OFV). The objective function is defined as

$$Minimize \ f = \frac{1}{nm \times nstep} \sum_{j=1}^{nstep} \sum_{i=1}^{nm} (h_{ij,sim} - h_{ij,mes})^2 \qquad (5)$$

where *nstep* is the number of the measured heads, *nm* is the number of observation wells, $h_{ij,sim}$ is the simulated head at *j*th time step at *i*th observation well, $h_{ij,mes}$ is the measured head at *j*th time step and at *i*th observation well. Now the initial solution is considered as the current optimal solution.

The third step is to generate a new trial solution based on equation (2). If the new trial solution is not within solution domain, the SA-MF has to randomly generate another one which falls within the solution domain. The fourth step is to simulate the hydraulic head distribution by MODFLOW-2000 with the trial solution and its corresponding OFV. With the OFV, the trial solution is checked to see whether this one is a new optimum or not is the fifth step. If the OFV of the trial solution is better than the current optimal solution or if the trial solution satisfies Metropolis's criterion, the current optimal solution is replaced with the trial solution in the sixth step. Otherwise, the algorithm will continue generating the new trial solution in seventh and eighth steps. The ninth and tenth steps are the same as those mentioned at the last paragraph in last section. In this study, the stopping criterion is chosen as if the absolute difference between the two OFVs obtained at two consecutive

temperatures is less than 10^{-6} four times successively.

CHAPTER 4   Results and Discussion

This section is divided into three parts.   The first part given in Section 4.1 is designed to test the performance of the proposed SA-MF on the homogeneous and isotropic confined aquifer.   The results are also used to summarize the requirements for effectively solving pumping source identification problem.   In the second part presented in Section 4.2, the SA-MF is used to identify the pumping source information on the homogeneous and isotropic unconfined aquifer.   Finally, two different type problems are considered to examine the performance of the SA-MF in Section 4.3.   In Section 4.3.1, the proposed SA-MF is used to analyze the pumping source information problems in heterogeneous formations representing possible real world aquifers.   In Section 4.3.2, the field test data are applied to examine the ability of SA-MF in real world problem.   Table 2 is the summary of the case studies designed in this study.

4.1 Applications to a homogeneous and isotropic confined aquifer

Four unknown variables: the source location of x and y coordinates, pumping rate, and pumping period are considered for solving the problem of pumping source information estimation.   Note that SA-MF determines the source location in terms of the x and y coordinates.   Four scenarios are contained in the first part.   Scenario 1 is

designed to verify the minimum requirement on the number of measured heads for

effectively solving the pumping source identification problem.   The examinations of

measurement error are also involved in this study.   The scenario 2 is to examine the

influence of measurement errors on the estimated results.   Scenario 3 is to find an

effective way to increase the identified accuracy when the measurement error level is

high.   Finally, determining the requirement of the number of observation wells for

the pumping source identification analysis is the main issue in the fourth scenario.

4.1.1 Hypothetic site description

An example of pumping in a homogenous and isotropic confined aquifer is used

for illustrating the pumping source identification procedure.   The aquifer length and

width are both 1000 m and the aquifer thickness is 20 m.   The top and bottom

elevations, hydraulic conductivity, porosity, and storage coefficient are 10.0 and -10.0

m, 5×10^{-6} m/s, 0.1, and 1×10^{-4}, respectively.   Figure 3 is the cross sectional view of

the hypothetic aquifer system.   The finite difference grids are block-centered and the

related boundary conditions for the aquifer system are shown in Figure 4.   The upper

and lower boundaries are specified as no flux boundaries and the left and right

boundaries are specified as constant head boundaries.   The elevations of the

hydraulic head at left and right boundaries are 30.0 and 20.0 m, respectively.   The

grid width and length are both 10 m; thus, the number of finite difference meshes is

100×100.   This example assumes that a pumping well P1 is located at (495 m, 495 m) and the pumping rate and pumping period are 200.0 CMD (m^3/day) and 60.0 minutes, respectively.   The measured heads at 15 observation wells indicated in Figure 4 are simulated using MODFLOW-2000 and listed in Table 3.   Notice that the drawdown at a distance of 500 m away from P1 is smaller than 0.001 m when the pumping rate is 200 CMD and the pumping period is less than 170 minutes based on the calculation using Theis solution [*Todd and Mays*, 2005].

All the nodal points are considered as the suspicious pumping source locations except those meshes containing the observation wells.   The upper bounds for the pumping rate and pumping period are set as 1000.0 CMD and 120.0 minutes, respectively, and the lower bounds are both given as zero.   The *NS*, *NT*, initial temperature, and R_{Te} are chosen as 20, 10, 5, and 0.8, respectively.   All initial guesses in the case studies are given by random number generator.

4.1.2   Case studies

The purpose of this scenario is to explore the required number of measured heads for solving the pumping source identification problem in a homogeneous and isotropic site.   Mathematically, at least four measured heads are needed to solve those four unknowns.   Eight cases are designed to investigate the influence of the number of measured heads on the results of pumping source estimation.

Four measured heads are used to estimate the pumping source information in cases 1-1 to 1-4 while five measured heads are used in cases 1-5 to 1-8. The analyzed results using four observations with different allocation of the observation wells are shown in Table 4. The estimated pumping locations are correctly determined at (495 m, 495 m) in cases 1-1, 1-2 and 1-4. Yet, the estimated location of (485 m, 505 m) in case 1-3 is incorrect. In cases 1-1, 1-2, and 1-4, the estimated pumping rates are respectively 200.99, 216.22, and 198.92 CMD and the estimated pumping periods are 54.22, 43.98, and 59.57 minutes, respectively. The largest relative errors are 8.11 % in the estimated pumping rate and 26.7 % in the estimated pumping period in case 1-2.
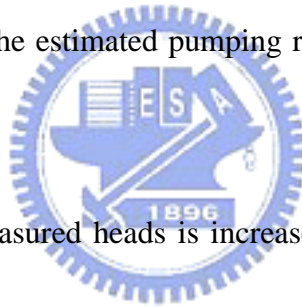
When the number of measured heads is increased to five, the estimated source locations for cases 1-5 to 1-8 are all correct and the estimated pumping rates and pumping periods are all close to the correct solutions. The largest relative errors are -1.89 % in the obtained pumping rate in case 1-7 and -2.3 % in the estimated pumping period in case 1-5. Obviously, one more measured head is useful in estimating pumping source information. Thus, the number of measured heads is suggest to be more than one at least to the number of unknown variables when solving the pumping source identification problem in a homogeneous and isotropic formation.

Scenario 2 considers that the measured heads have measurement error. The

25

disturbed measured head with random noise is expressed as

$$h'_{i,obs} = h_{i,obs} \times (1 + Er \times RD_3) \tag{6}$$

where $h'_{i,obs}$ is the disturbed measured head, Er is the level of measurement error, and

RD_3 is a random standard normal deviate generated by the routine RNNOF of IMSL

[2003]. Three different values of Er, 1 cm, 2 cm, and 3 cm, are chosen in this

scenario and ten runs are performed for each level of measurement error. The

estimated results shown in Table 5 indicate that the source locations are correctly

identified when the values of Er are 1 cm and 2 cm. The average of estimated

pumping rate and pumping period are respectively 199.42 CMD and 60.41 minutes.

The largest relative error is -1.24 % in the estimated pumping rate and 3.72 % in the

estimated pumping period in case 2-2 as Er is 1 cm. In addition, the average of the

estimated pumping rate and pumping period are respectively 199.24 CMD and 60.64

minutes. The largest relative error is -2.84 % in the estimated pumping rate and

11.55 % in the estimated pumping period in case 2-20 as Er is 2 cm. However, as

the measurement error level increases to 3 cm, only six out of ten runs obtain the

correct source location as indicated in Table 5. The average of the estimated

pumping rate and pumping period in those six runs are respectively 200.09 CMD and

60.20 minutes. The largest relative error is 3.65 % in the estimated pumping rate

and -9.28 % in estimated pumping period in case 2-30 as Er is 3 cm.

Based on the results obtained in scenario 2, the estimated pumping source location, pumping rate, and/or pumping period may be incorrect as the level of measurement error is high. Accordingly, cases 3-1 to 3-8 are designed to find an effective way to increase the accuracy of the identified result as the measurement error level is high. In cases 3-1 to 3-4, the measured heads are taken from five different observation wells. Cases 3-5 to 3-6 and cases 3-7 to 3-8 are respectively used six and seven measured heads to estimate the pumping information. Table 6 lists the results obtained by the measured heads measured at the observation wells located at six different average distances respect to the pumping source. All the measured heads have the measurement error with the maximum Er of 3 cm. The estimated pumping source location, pumping rate, and pumping period are correct in cases 3-1 and 3-2. The accuracy of the results decreases as the average distance from the observation wells increases as indicated in the cases 3-3 and 3-4. However, as the number of the measured heads increases to six or seven, the pumping source location, pumping rate, and pumping period are all correctly determined in cases 3-5 and 3-8 as indicated in Table 6. Therefore, if the level of measurement error is high, the best way to obtain good identified results is to employ more measurement data in the pumping source estimation.

Twenty-three case studies in the scenario 4 are designed to examine the effect of

using the observations measured at two different time steps on the estimation for the pumping source information and the results are listed in Table 7.   In cases 4-1 to 4-3, eight observations measured at four wells are used to determine the pumping information.   While in cases 4-4 to 4-11, six observations measured at three wells and four observations measured at two wells in cases 4-12 to 4-23 are utilized.   As the number of observation wells is four or three, the determined pumping source location, pumping rate, and pumping period are correctly.   However, when the number of observation wells is two, only eight out of 12 runs yield the correct source location, pumping rate, and pumping period.   When a well is pumped, water is removed from the aquifer surrounding the well and the hydraulic surface forms a conic shape called cone of depression.   Since three points construct a plane, the number of observation wells should be at least three least for estimating the pumping source information.
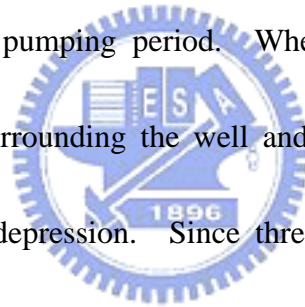
4.2 Applications to a homogeneous and isotropic unconfined aquifer

The proposed SA-MF is now used to examine the performance on a homogenous and isotropic unconfined aquifer in the second part.   The sectional view and plan view of the hypothetic unconfined aquifer system are respectively shown in Figure 3 and Figure 4.   As indicated in Figure 3, the top and bottom elevations of the unconfined aquifer are 50.0 and 10.0 m, respectively.   The elevations of the

28

hydraulic head at left and right boundaries are respectively specified as 40.0 and 30.0

m. And the hydraulic conductivity and specific yield are respectively 5×10^{-5} m/s

and 0.1. The pumping well P1 is also located at (495 m, 495 m) but the pumping

rate and period are respectively 1200.0 CMD and 8 hours. The measured heads,

simulated by the MODFLOW-2000 with the specific hydorgeologoic parameters and

boundary conditions, are listed in Table 8.

Scenario 5 contains four case studies and the measured heads used to estimate

the pumping source information are without considering the measurement error.

Case 5-1 chooses N-1, W-1, S-1, E-1, and E-2 as the observation wells for estimating

the pumping source information. Case 5-2 selects N-1, N-2, W-2, S-2, and E-2 as

the observation wells. In addition, cases 5-3 and 5-4 consider N-1, N-2, W-1, S-2,

and E-2 and N-2, W-2, S-1, E-1, and E-2, respectively, as the observation wells used

to estimate the pumping source information. The upper bound value for pumping

rate, pumping period, NS, NT, initial temperature, and R_{Te} used in SA are respectively

2400.0 CMD, 16 hours, 20, 10, 5, and 0.8.

The estimated pumping source locations are correctly determined at (495 m, 495

m) as indicated in Table 9. The average estimated pumping rate and period are

respectively 1200.33 CMD and 7.99 hours. The largest relative errors in the

estimated pumping rate and estimated pumping period are respectively -0.21 % and 1

% in case 5-2.

4.3 Applications to heterogeneous aquifer and field pumping test

data

This section is to estimate the pumping source information for problems with heterogeneous formation representing possible real-world aquifers. This section contains three categories. Three scenarios, i.e. scenarios 6 to 8, the hydraulic conductivity field is assumed to be perfectly known to estimate the pumping source information. Accordingly, it means the hydraulic conductivity fields used for generating the measured heads and estimating pumping source information are the same. Additionally, scenario 9 is designed to test the effect of the identified result on the observation well distribution. Three scenarios, i.e., scenarios 10 to 12, with different degree of variation of the random hydraulic conductivity fields and conditioning conductivity data in the problems are considered. Finally, the last category, i.e., scenario 13, considers using SA-MF and the measured heads obtained from the field experiment to estimate the pumping source information.

4.3.1   Heterogeneous and isotropic confined aquifer

Field aquifer tests such as slug test or pumping test are usually used to determine hydrogeologic parameters, i.e., hydraulic conductivity and storativity. These aquifer

parameters obtained at specific locations can be used as conditioning information. The heterogeneous nature of aquifers may be characterized by three statistical parameters: the mean hydraulic conductivity, the variance in hydraulic conductivity, and the correlation length. Therefore, the hypothetic heterogeneous formations have random hydraulic conductivity fields which are spatially-correlated and log-normally distributed. The correlation lengths (λ) in both *x* and *y* coordinates are chosen as 100 m and the mean of the logarithm hydraulic conductivity (*lnK*) are -12.206 m/s. The mean and standard deviation of *lnK* are denoted as $\bar{y}$ and σ_y, respectively, where y = *lnK*. Three different values of σ_y, including 0.5, 1.0, and 1.5 m/s, representing different level of aquifer heterogeneity are considered. All the conductivity fields are generated by the program SASIM of the geostatistical software, GSLIB [*Deutsch and Journel*, 1998]. The SASIM can produce spatially-correlated conductivity fields with preserving the known mean and variance of *lnK* and known values at specific locations. The dimensions of the hypothetic aquifer are the same as those given in the section 4.1, i.e., the length and width are both 1000 m and the aquifer thickness is 20 m. The locations of pumping source and observation wells are depicted in Figure 4.

4.3.1.1 The hydraulic conductivity field is perfectly known

In this section, containing three scenarios and 12 case studies for each scenario,

the hydraulic conductivity field is assumed to be perfectly known while estimating the

pumping source information.   Accordingly, it means the hydraulic conductivity

fields in generating the measured heads process and in estimating pumping source

process are the same.   The values of σ_y in scenarios 6 to 8 are 0.5, 1.0, and 1.5,

respectively.

Four sets of hydraulic conductivity obtained from three sets of observation well

locations are designed to examine the performance of SA-MF on heterogeneous

aquifer analysis.   Each set of observation well locations involves four observation

wells.   The observation well locations are chosen as N-1, W-1, S-1, and E-1 in case

6-1 to 6-4, 7-1 to 7-4, and 8-1 to 8-4.   Cases 6-5 to 6-8, 7-5 to 7-8, and 8-5 to 8-8

choose four observation wells at N-2, W-2, S-2, and E-2.   The observation wells are

located at NW-1, SW-1, SE-1, and NE-1 in cases 6-9 to 6-12, 7-9 to 7-12, and 8-9 to

8-12.   Table 10 lists the hydraulic conductivities obtained from a field aquifer test

and the measured heads simulated by MODFLOW-2000 with the pumping rate and

period of 200.0 CMD and 60.0 minutes, respectively.   Accordingly, Table 11 and

Table 12 list the hydraulic conductivities and measured heads as the σ_y are 1.0 and 1.5

m/s, respectively.   Note that all the average lnK for each set of hydraulic

conductivities are -12.206 m/s.

Table 13 lists the results while the hydraulic conductivity field is perfectly

known in pumping source information estimation. All obtained pumping source locations are correctly identified at (495 m, 495 m). The average estimated pumping rate and period are respectively 199.87 CMD and 59.98 minutes while the value of σ_y is 0.5 m/s. The largest relative error is -0.06 % in the estimated pumping rate in case 6-4 and -0.03 % in the estimated pumping period in case 6-6. In scenario 7, the average estimated pumping rate and pumping period are respective 199.87 CMD and 60.00 minutes. The largest relative errors in the estimated pumping rate and pumping period are -0.06 % in case 7-8 and 0.01 % in case 7-7, respectively. While the value of σ_y increases to 1.5 m/s, the average estimated pumping rate and pumping period are respective 199.90 CMD and 59.97 minutes. The largest relative errors in the estimated pumping rate and pumping period are -0.05 % in case 8-9 and -0.05 % in case 8-2, respectively.

Additionally, scenario 9 containing seven case studies is designed to examine the effect of the distribution of the monitoring wells on the estimated result. Among each case study, six measured heads obtained at three observations at two different time steps are used to estimate the pumping source information. Cases 9-1 to 9-4 select three monitoring wells located at downgradient from the pumping source. The monitoring wells are also located at upgradient to the pumping source in cases 9-5 to 9-7 for comparison. Notice that the pumping source is not located within the area

encompassed by the selected monitoring wells. All the pumping source locations are correctly estimated as indicated in Table 14. The average estimated pumping rate and pumping period are respectively 199.94 CMD and 60.05 minutes. The largest relative errors in the estimated pumping rate and pumping period are -0.19 % and 0.33 % in case 9-4, respectively. Therefore, the distribution of selected monitoring wells is not an essential requirement for effectively estimating pumping source information.

4.3.1.2 The hydraulic conductivity fields are generated by conditional

simulation

Scenarios 10 to 12 are to test the performance of SA-MF on a priori knowledge of the statistical parameters to the flow field. Three standard deviations of the natural logarithm of hydraulic conductivity and three sets of observation well locations are considered. Table 15 lists the hydraulic conductivities obtained from the field aquifer test and the measured heads simulated by MODFLOW-2000 with the pumping rate and period of 200.0 CMD and 60.0 minutes, respectively. Note that the observation wells are the same as those in scenarios 10 to 12. The observation wells are located at N-1, W-1, S-1, and E-1. Another fifty realizations of random conductivity fields and the proposed method are employed along with these eight measured heads to estimate the pumping source information.

The pumping sources are all correctly estimated at (495 m, 495 m) in scenarios

10 to 12.　Figures 5 to 7 show the estimated pumping rate and pumping period while the values of σ_y are 0.5, 1.0 and 1.5 m/s.　The average estimated pumping rate and pumping period are respectively 197.11 CMD and 61.11 minutes while the value of σ_y is 0.5 m/s.　The standard deviation of the estimated pumping rate and pumping period are respectively 5.53 CMD and 4.48 minutes.　The largest relative errors in the estimated pumping rate and pumping period are -7.09 % in case 10-35 and 22.69 % in case 10-4, respectively.　In scenario 11, the average estimated pumping rate and pumping period are respective 193.74 CMD and 63.37 minutes.　The standard deviation of the estimated pumping rate and pumping period are respectively 9.39 CMD and 8.63 minutes.　The largest relative errors in the estimated pumping rate and pumping period are -11.06 % in case 11-6 and 38.01 % in case 11-33, respectively. While the value of σ_y increases to 1.5 m/s, the average estimated pumping rate and pumping period are respective 188.02 CMD and 65.23 minutes.　The standard deviation of the estimated pumping rate and pumping period are respectively 10.59 CMD and 7.88 minutes.　The largest relative errors in the estimated pumping rate and pumping period are -16.07 % and 38.52 % in case 12-40, respectively. Obviously, the accuracy of the estimated pumping rate and pumping period is decreased with increasing the value of σ_y.

4.3.2   Field case study

The last scenario, scenario 13, the data from a field pumping test is used to estimate the pumping source information.   The field experiment was performed at the north eastern corner of Taiwan in 1987.   Figure 8 is the plan view of Yenliao site. The dimension of the aquifer system is 200 m in both length and width.   One pumping well, denoted as P, and four observation wells, denoted as A to D, are used for the field experiment.   The pumping well is located at (97.5 m, 97.5 m).   The distances between observation wells to pumping well are 5 m for A, 10 m for B, and 20 m for C and D.   According to the drill log obtained at P, the stratum formation could be divided into five layers.   The first layer is yellow brown sandy soil ranging from the ground surface to the depth of 1.7 m.   The second layer is bluish gray sandy shale between 1.7 m to 4.2 m under the ground surface.   The third layer is fine to medium grained sand stone, ranging from 4.2 m to 7.8 m under the ground surface, and the fourth layer is bluish gray shale intercalated with sand stone, from the depth of 7.8 m to the depth of 11.4 m.   The last layer is dark gray shale occasionally with sandstone between 11.4 m to 16.0 m under the ground surface.   Therefore, the aquifer thickness is assumed as 16 m.

According to the field investigation, the topography is flat and the gradient of the ground surface is about 0.01.   The piezometric surface is at the depth of 1 m under

the ground surface. The groundwater flows toward north-east, the upper and lower

boundaries are assumed as no-flow boundary and the left and right boundaries are

considered as constant head boundary. The elevations of the hydraulic head at left

and right boundaries are respectively 17 m and 15 m. The grid width and length are

both 2.5 m; thus, the number of finite difference mesh is 80×80. The aquifer

system is assumed as isotropic. All the pumping well and observation wells are fully

penetrated through the aquifer thickness. The conductivity field could be divided

into two zones based on the result from the field experiment. The estimated

transmissivity and storage coefficient are respectively 3.9 m^2/day and 3.73 $\times 10^{-4}$ in

the zone 1 as indicated in Figure 8. The transmissivity and storage coefficient are

20.51 m^2/day and 3.83 $\times 10^{-3}$ in the zone 2, respectively. Figure 9 shows the cross

sectional view of the confined aquifer system at Yenliao site. Table 16 lists the

drawdown data and the locations of the pumping well and observation wells. The

drawdown data were measured at the pumping periods 10 and 20 minutes and the

pumping rate was 10 L/min.

All the nodal points inside the problem domain are considered as the suspicious

pumping source locations except those nodes contain the observation well. The

upper bounds for the pumping rate and pumping period are set as 100.0 L/min and

60.0 minutes, respectively, and the lower bounds are both given as zero. The *NS*, *NT*,

initial temperature, and R_{Te} are chosen as 20, 10, 5, and 0.8, respectively.   All initial

guesses in the case studies are given by random number generator.

Four case studies are used to test the performance of the SA-MF for a real

problem.   Table 17 lists the observation wells used in these four cases for the

estimation and the identified results by SA-MF.   The estimated source locations are

all correct at (97.5 m, 97.5 m) in cases 13-1 to 13-4.   The average estimated pumping

rate and pumping period are respectively 10.43 L/min and 19.14 minutes.   The

largest relative errors in the estimated pumping rate and pumping period are 7.3% and

-5.65% in case 13-2, respectively.   Therefore, the proposed SA-MF is applicable to

the field problem for estimating the pumping source information.
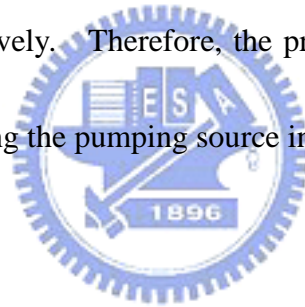
CHAPTER 5 Conclusions

Groundwater resource is a precious natural water resource. While the available freshwater is short, the groundwater resource can provide significant quantity water to satisfy the domestic or industrial usage. Therefore, the groundwater resource usually is not allowed to pump for public or private usage without permit. Illegal pumping may have negative impacts on the groundwater flow system and impair the quantity and quality of the groundwater of a remediation site. Thus, development of a methodology for estimating the pumping source estimation is necessary for protecting the groundwater resource.

A new approach, SA-MF, is developed to incorporate a three-dimensional groundwater flow, MODFLOW-2000, with SA for solving the pumping source identification problem. In this approach, SA is employed to generate the trial solutions, i.e., pumping source location, pumping rate, and pumping period. Then the MODFLOW-2000 is employed to simulate the hydraulic heads at the observation wells. In this study, all the initial guesses are generated by the random number generator.

Thirteen scenarios are designed to test the performance of SA-MF on homogeneous or heterogeneous aquifer systems. Scenarios 1 to 4 consider the aquifer system as a homogeneous and isotropic confined aquifer. Scenario 5 is to

test the performance of SA-MF on the homogeneous and isotropic unconfined aquifer

system. Scenarios 6 to 12 consider a heterogeneous and isotropic confined

formation to represent possible real-world aquifer systems. The hydraulic

conductivity fields are assumed to be known for estimating the pumping source

information in scenarios 6 to 8. Scenario 9, which contains seven case studies, is to

examine the effect of the distribution of the monitoring wells on the estimated results.

Scenarios 10 to 12 use Monte Carlo simulation to estimate the pumping source

information while the hydraulic conductivity fields are generated by conditional

simulation. In the last scenario, i.e., scenario 13, a field pumping test data is used to

examine the performance of SA-MF. The requirement of the number of observation

wells for effectively estimating source information is also studies. Six conclusions

can be drawn as follows.
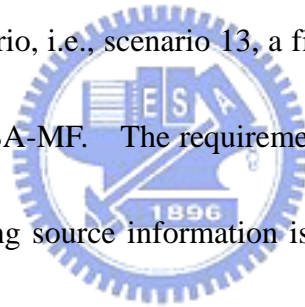
First, the approach we developed can be used to solve the pumping source

information estimation problem for a synthetic homogeneous/ heterogeneous aquifer

or a field aquifer system and the estimated results are accurate. Second, the

proposed approach can obtain accurate results even the initial guesses for the SA

parameters and pumping source information are generated by a random number

generator. Third, five measured heads at least should be used to analyze the

pumping source estimation problem. Fourth, three observation wells at least are

required for effectively identifying the pumping source location, pumping rate, and

pumping period.   The location of monitoring wells is not important in estimating the

pumping source information.   Fifth, when the level of measurement error is high, the

best way to correctively estimate the pumping source information is to increase the

number of measured heads.   Finally, the proposed approach is applicable even the

measured heads contain measurement error level up to 3 cm.

Reference

Aral, M.M., and J. Guan (1996), Genetic algorithms in search of groundwater pollution sources, in *Advances in Groundwater Pollution Control and Remediation,* NATO ASI Series 2 Environment, Kluwer Academic Publishers, The Netherlands, 9, 347-369.

Aral, M.M., J. Guan, and M.L. Maslia (2001), Identification of contaminant source location and modflow-gwt release history in aquifers, *J of Hydrologic Engineering*, *6*(3), 225-234.

Atmadja, J., and A.C. Bagtzoglou (2001), State of the art report on mathematical methods for groundwater pollution source identification, *Environ. Forensics*, *2*, 205-214.

Bagtzoglou, A.C., D.E. Kougherty, and A.F.B. Tompson (1992), Applications of particle methods to reliable identification of groundwater pollution sources, *Water Resour. Manage.*, *6*, 15-23.

Bear, J. (1979), *Hydraulics of Groundwater*, 567 pp., McGraw-Hill, New York.

Cai, X., D.C. McKinney, and L.S. Lasdon (2001), Solving nonlinear water management models using a combined genetic algorithm and linear programming approach, *Adv. Water Resour.*, *24*(6), 667-676.

Cooper, V.A., V.T.V. Nguyen, and J.A. Nicell (1997), Evaluation of global optimization methods for conceptual rainfall-runoff model calibration, *Wat. Sci. Tech.*, *36*(5), 53-60.

Corana, A., M. Marchesi, C. Martini, and S. Ridella (1987), Minimizing multimodal function of continuous variables with the simulated annealing algorithm, *ACM Transactions on Mathematical Software*, *13*, 262-280.

Cunha, M.D.C., and J. Sousa (1999), Water distribution network design optimization: simulated annealing approach, *J. Water Resour. Plng. Manage.*, *125*(4), 215-221.

Doutherty, D.E., and R.A. Marryott (1991), Optimal groundwater management: I. Simulated annealing, *Water Resour. Res.*, *27*(10), 2493-2508.

Deutsch, C.V., and A.G. Journel (1998), *GSLIB: Geostatistical Software Library and User's Guide*, 2nd ed, Oxford Univ. Press, New York.

Goffe, W.L., G.D. Ferrier, and J. Rogers (1994), Global optimization of statistical functions with simulated annealing, *Journal of Econometrics*, *60*(1), 65-100.

Gorelick, S. M., B. Evans, and I. Remson (1983), Identifying sources of groundwater pollution: An optimization approach, *Water Resour. Res.*, *19*(3) 779-790.

Guo, J.Q., and L. Zheng (2005), A modified simulated annealing algorithm for estimating solute transport parameters in streams from tracer experiment data, *Environmental Modeling and Software*, *20*(6), 811-815

Habib, Y., M.S. Sadiq, and A. Hakim (2001), Evolutionary algorithms, simulated annealing and tabu search: a comparative study, *Engineering Applications of Artificial Intelligence*, *14*, 167-181.

Harbaugh, A.W., E.R. Banta, M.C. Hill, and M.G. McDonald (2000), MODFLOW-2000, The U.S. Geological survey modular ground-water model-user guide to modularization concepts and the ground-water process, *Open File Report 00-92*, 121 pp., U.S. Geological Survey, Reston, VA.

Hwang, J.C., and R.M. Koerner (1983), Groundwater pollution source identification from limited monitoring well data: part I – theory and feasibility, *J. of Hazardous Materials*, *8*, 105-119.
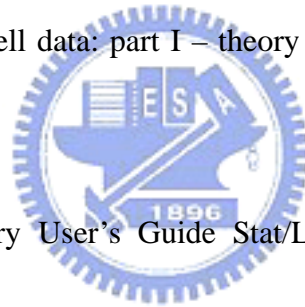
IMSL (2003), Fortran Library User's Guide Stat/Library*, Volume 2 of 2*, Visual Numerics Inc., Houston, TX.

Jeong, I.K., and J.J. Lee (1996), Adaptive simulated annealing genetic algorithm for system identification, *Engng Applic. Artif. Intell.*, *9*(5), 523-532.

Kuo, C.H., A.N. Michel, and W.G. Gray (1992), Design of optimal pump-and-treat strategies for contaminated groundwater remediation system using the simulated annealing algorithm, *Adv. Water Resour.*, *15*(2), 95-105.

Kirkpatrick, S., C.D. Jr. Gelatt CD, and M.P. Vecchi (1983), Optimization by simulated annealing, *Science*, *220*(4598), 671-680

Li, L., D.A. Barry, J. Morris, and F. Stagnitti (1999), CXTANNEAL: an improved program for estimating solute transport parameters, *Environmental Modelling and Software with Environment Data News*, *14*(6), 607-611.

Lin, Y.C., and H.D. Yeh (2005), THM species forecast using optimization method: genetic algorithm and simulated annealing, *J. Comput. Civ. Eng.*, *19*(3), 248-257.

Liu, C., and W.P. Ball (1999), Application of inverse methods to contaminant source identification from aquitard diffusion profiles at Dover AFB, Delaware, *Water Resour. Res.*, *35*(7), 1975-1985.

Loáiciga, H.A. (2004), Analytic game-theoretic approach to ground-water extraction, *J. Hydrol.*, *297*, 22-33.

Mahar, P.S., and B. Datta (1997), Optimal monitoring network and ground-water pollution source identification, *J. Water Resour. Plng. Manage.*, *123*(4), 199-207.

Mahar, P.S., and B. Datta (2000), Identification of pollution sources in transient groundwater systems, *Water Res. Manage.*, *14*(3), 209-227.

Mahar, P.S., and B. Datta (2001), Optimal identification of groundwater pollution sources and parameter estimation, *J. Water Resour. Plng. Manage.*, *127*(1), 20-29.

Mahinthakumar, G., and M. Sayeed (2005), Hybrid genetic algorithm-local search methods for solving groundwater source identification inverse problem, *J. Water Resour. Plng. Manage.*, *131*(1), 45-57.

Mahinthakumar, G.., and M. Sayeed (2006), Reconstructing groundwater source release histories using hybrid optimization approaches, *Environ. Forensics*, *7*(1), 45-54.

Marryott, R.A. (1996), Optimal ground-water remediation design using multiple control technologies, *Ground Water*, *34*(3), 425-433.

Marryott, R.A., D.E. Dougherty, and R.L. Stollar (1993), Optimal groundwater management: 2. Application of simulated annealing to a field-scale contaminant site, *Water Resour. Res.*, *29*(4), 847-860.
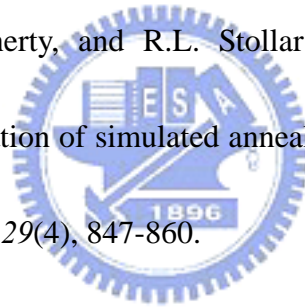
McDonald, M.G., and A.W. Harbaugh (1988), A modular three-dimensional finite-difference ground-water flow model, *Book 6*, 586 pp., Techniques of Water Resources Investigations of the U.S. Geological Survey, Reston, VA.

Metropolis, N., A.W. Rosenbluth, M.N. Rosenbluth, A.H. Teller, and E. Teller (1953), Equation of state calculations by fast computing machines, *Journal of Chemical Physics.*, *21*(6):1087-1092.

Monem, M.J., and R. Namdarian (2005), Application of simulated annealing (SA) techniques for optimal water distribution in irrigation canals, *Irrigation and*

Drainage, *54*(4), 365-373.

National Research Council (1990), *Groundwater Models – Scientific and Regulatory Applications*, National Academy Press, Washington D.C.

Neupauer, R.M., and J.L. Wilson (1999), Adjoint method for obtaining backward-in-time location and travel time probabilities of a conservative groundwater contaminant, *Water Resour. Res.*, *35*(11), 3389-3398.

Neupauer, R.M., and J.L. Wilson (2001) Adjoint-derived location and travel time probabilities for a multi-dimensional groundwater system, *Water Resour. Res.*, *37*(6), 1657-1668.

Neupauer, R.M., B. Borchers, and J.L. Wilson (2000), Comparison of inverse methods for reconstructing the release history of a groundwater contamination source, *Water Resour. Res.*, *36*(9), 2469-2475.
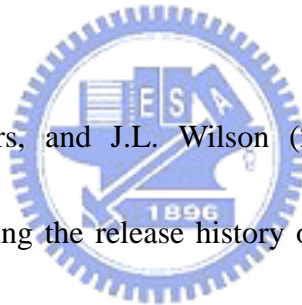
Pham, D.T., and D. Karaboga (2000), *Intelligent Optimization Techniques: Genetic Algorithm, Tabu Search, Simulated Annealing and Neural Network*, 302 pp., Springer-Verlag, New York.

Rayward-Simith, V.J., I.H. Osman, C.R. Reeves, and G.D. Smith (1996). *Modern heuristic search methods*, John Wiley and Sons, NY.

Rizzo, D.M., D.E. Dougherty (1996), Design optimization for multiple period groundwater remediation, *Water Resour. Res.*, *32*(8), 2549-2561.

Romeo, F., and A. Sangiovanni-Vincentelli (1991), A theoretical framework for simulated annealing, *Algorithmica*, *6*(3), 302-345.

Sayeed, M., and G. Mahinthakumar (2005), Efficient parallel implementation of hybrid optimization approaches for solving groundwater inverse problems, *J. Comput. Civ. Eng.*, *19*(4), 329-340.

Sciortino, A., T.-C. Harmon, and W. W-G Yeh (2000), Inverse modeling for location dense nonaqueous pools in groundwater under steady flow conditions, *Water Resour. Res.*, *36*(7), 1723-1735.

Shieh, H.-J., and R.C. Peralta (2005), Optimal in situ bioremediation design by hybrid genetic algorithm-simulated annealing, *J. Water Resour. Plan. Manage.*, *131*(1), 67-78.
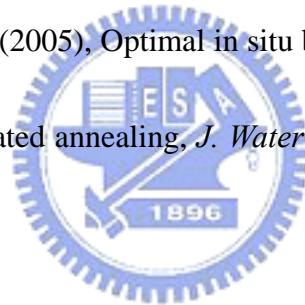
Skaggs, T.H., and Z.J. Kabala (1994), Recovering the release history of a groundwater contaminant, *Water Resour. Res.*, *30*(1), 71-79.

Skaggs, T.H., and Z.J. Kabala (1995), Recovering the history of a groundwater contaminant plume: Method of quasi-reversibility, *Water Resour. Res.*, *31*(11), 2669-2673.

Skaggs, T.H., and Z.J. Kabala (1998), Limitations in recovering the history of a groundwater contaminant plume, *J. Contam. Hydrol.*, 33, 347-359.

Snodgrass, M.F., and P.K. Kitanidis (1997), A geostatistical approach to contaminant

source identification, *Water Resour. Res.*, *33*(4), 537-546.

Todd, D.K, and L.W. Mays (2005), *Groundwater Hydrology*, 3rd ed., 636 pp., Wiley, NJ.

Tung, C.P., C.C. Tang, Y.P. Lin. (2003), Improving groundwater flow modeling using optimal zoning methods, *Environmental Geology*, *44*, 627-638.

Wagner, B.J., (1992), Simultaneous parameter estimation and contaminant source characterization for coupled groundwater flow and contaminant transport modeling, *J. Hydrol., 135*, 275-303.

Woodbury, A., E. Sudicky, T.J. Ulrych, and R. Ludwig (1998), Three-dimensional plume source reconstruction using minimum relative entropy inversion, *J. Contam. Hydrol.*, *32*, 131-158.
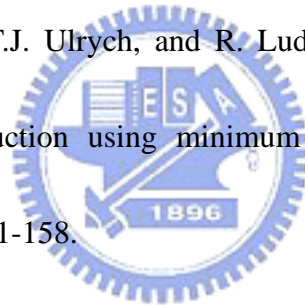
Woodbury, A.D., and T.J. Ulrych (1996), Minimum relative entropy inversion: theory and application to recovering the release history of a groundwater contaminant, *Water Resour. Res.*, *32*(9), 2671-2681.

Yeh, H.D., <u>Y.C. Lin</u>, and Y.C. Huang (2005), Application of simulated annealing and genetic algorithm for identifying leaky aquifer parameters, *Hydrological process*. (in press)

Zheng, C., and P. Wang (1996), Parameter structure identification using tabu search and simulated annealing, *Adv. Water Resour.*, *19*(4), 215-224.

Table 1 Process, packages, and additional capabilities of MODFLOW-2000 (Version 1.1, 1/17/2001)

Process	Packages	Additional capabilities
GWF1: Groundwater flow process	ADV2: Advective-transport observation package	HYDMOD-Hydrograph option
OBS1: Observation process	BAS6: Basic package	
PES1: Parameter estimation process	BCF6: Block centered flow package	
	CHD6: Time variant specified head package	
	DE45: Direct solver	
	DRN6: Drain package	
	DRT1: Drains with return flow package	
	EVT6: Evapotransipiration package	
	ETS1: Evapotranspiration with segmented function package	
	FHB1: Flow and head boundary package	
	GHB6: General head boundary package	
	HFB6: Horizontal flow barrier package	
	HUF1: Hydrogeologic-unit flow package	
	IBS6: Interbed storage package	
	LAK3: Leakage package	
	LPF1: Layer property flow package	
	PCG2: Version 2 of preconditioned conjugate gradient package	
	RCH6: Recharge package	
	RES1: Reservoir package	
	RIV6: River package	
	SIP5: Strongly implicit procedure package	
	SOR5: Slice successive over relaxation package	
	STR6: Streamflow-routing package	
	Wel6: Well package	

Table 2 The summary of designed case studies

Scenario description	Case studies	Results
Part 1: Homogeneous and isotropic aquifer analysis		
1. Determine the number of measured heads needed	8	Table 4
2. Examine the performance on measurement error	30	Table 5
3. Improve the performance as measurement contains error	8	Table 6
4. Determine the number of observation wells needed	23	Table 7
Part 2: Homogeneous and isotropic unconfined aquifer analysis		
5. Test the performance on the homogeneous unconfined aquifer	4	Table 9
Part 3: Heterogeneous and isotropic confined aquifer analysis		
6. Test the performance on flow fields that are perfectly known with σ_y 0.5	12	Table 13
7. Test the performance on flow fields that are perfectly known with σ_y 1.0	12	
8. Test the performance on flow fields that are perfectly known with σ_y 1.5	12	
9. Test the performance on the monitoring wells distribution	7	Table 14
10. Test the performance on the flow fields that are generated by conditional simulation with σ_y 0.5	50	Figure 5
11. Test the performance on the flow fields that are generated by conditional simulation with σ_y 1.0	50	Figure 6
12. Test the performance on the flow fields that are generated by conditional simulation with σ_y 1.5	50	Figure 7
13. Test the performance with the field test data	4	Table 17

Table 3 The location and observed hydraulic head at observed wells for homogeneous and isotropic confined aquifer

Observation wells	Location	Measured heads(m)		
		Initial state	Pumping period	
			T = 30 (min)	T = 60 (min)
N-1	(465 m, 495 m)	25.041	22.621	21.275
N-2	(395 m, 495 m)	25.040	24.769	24.388
NW-1	(395 m, 395 m)	26.031	25.945	25.781
NW-2	(295 m, 295 m)	27.023	27.02	27.013
W-1	(495 m, 425 m)	25.734	25.086	24.408
W-2	(495 m, 395 m)	26.031	25.759	25.378
SW-1	(595 m, 395 m)	26.031	25.945	25.781
SW-2	(695 m, 295 m)	27.022	27.020	27.012
S-1	(585 m, 495 m)	25.040	24.680	24.216
S-2	(595 m, 495 m)	25.040	24.769	24.388
SE-1	(595 m, 595 m)	24.051	23.965	23.801
E-1	(495 m, 535 m)	24.645	22.958	21.809
E-2	(495 m, 595 m)	24.051	23.779	23.398
E-3	(495 m, 695 m)	23.062	23.043	22.995
NE-1	(395 m, 595 m)	24.050	23.964	23.800

Table 4 The identified results with the observations without considering measurement error and the pumping period is unknown

Case	Number of measured head	Observation wells	Identified results		
			Source location	Pumping rate (CMD)	Pumping period (min)
1-1	4	N-1, W-1, S-1, E-1	(495 m, 495 m)	200.99	54.22
1-2		N-2, W-2, S-2, E-2	(495 m, 495 m)	216.22	43.98
1-3		NW-1, SW-1, SE-1, NE-1	*(485 m, 505 m)*	*226.90*	*72.42*
1-4		NW-2, SW-2, E-3, E-1	(495 m, 495 m)	198.92	59.57
1-5	5	N-1, W-1, S-1, S-2, E-1	(495 m, 495 m)	200.21	58.62
1-6		N-1, N-2, W-2, S-2, E-2	(495 m, 495 m)	198.73	60.02
1-7		NW-1, SW-1, SE-1, E-2, NE-1	(495 m, 495 m)	196.22	61.26
1-8		NW-2, SW-2, E-2, E-3, E-1	(495 m, 495 m)	198.99	60.38

Note that the pumping source is located at (495 m, 495 m) and the pumping rate and pumping period are is 200 CMD and 60 minutes respectively.

Table 5 The identified results while the measurement containing error

| Case | Identified results | | |
	Source location	Pumping rate (CMD)	Pumping period (min)
Maximum error = 1 cm			
2-1	(495 m, 495 m)	198.42	60.54
2-2	(495 m, 495 m)	197.53	62.23
2-3	(495 m, 495 m)	200.12	60.08
2-4	(495 m, 495 m)	199.43	60.12
2-5	(495 m, 495 m)	200.63	59.93
2-6	(495 m, 495 m)	198.12	61.12
2-7	(495 m, 495 m)	198.96	60.43
2-8	(495 m, 495 m)	200.72	59.21
2-9	(495 m, 495 m)	198.43	61.73
2-10	(495 m, 495 m)	201.87	58.75
Maximum error = 2 cm			
2-11	(495 m, 495 m)	197.32	61.21
2-12	(495 m, 495 m)	200.88	59.83
2-13	(495 m, 495 m)	201.32	58.76
2-14	(495 m, 495 m)	199.08	60.19
2-15	(495 m, 495 m)	203.43	56.42
2-16	(495 m, 495 m)	196.43	62.48
2-17	(495 m, 495 m)	197.83	62.13
2-18	(495 m, 495 m)	203.53	56.83
2-19	(495 m, 495 m)	198.21	61.63
2-20	(495 m, 495 m)	194.32	66.93
Maximum error = 3 cm			
2-21	(495 m, 495 m)	198.50	61.42
2-22	*(505 m, 505 m)*	*205.51*	*54.32*
2-23	*(505 m, 505 m)*	*199.23*	*60.45*
2-24	(495 m, 495 m)	202.67	58.48
2-25	*(495 m, 505 m)*	*200.68*	*60.43*
2-26	(495 m, 495 m)	204.13	55.46
2-27	(495 m, 495 m)	193.98	66.43
2-28	(495 m, 495 m)	194.15	64.98
2-29	*(505 m, 495 m)*	*203.12*	*62.30*
2-30	(495 m, 495 m)	207.13	54.43

Note that the measured heads measured at four different observation wells, N-1, W-1, S-1, S-2 and E-1, are used for determining the source location and pumping rate in these ten test runs. The pumping source is located at (495 m, 495 m) and the pumping rate and period are respectively 200 CMD minutes.

Table 6 The effect between the identified result and the observation wells at different average distance with the maximum measurement error is 3 cm

Case	Observation wells	Average distance (m)	Identified results		
			Source location	Pumping rate (CMD)	Pumping period (min)
3-1	N-1, W-1, S-1, S-2, E-1	66.0	(495 m, 495 m)	198.50	61.42
3-2	N-1, N-2, W-2, S-2, E-2	86.0	(495 m, 495 m)	197.26	62.38
3-3	NW-1, SW-1, SW-2, SE-1, NE-1	169.7	*(505 m, 485 m)*	*195.18*	*64.29*
3-4	NW-2, SW-2, E-1, E-2, E-3	181.1	*(455 m, 545 m)*	*208.31*	*50.41*
3-5	NW-1, SW-1, S-2,SE-1, NE-1, E-2	120.5	(495 m, 495 m)	198.76	61.18
3-6	NW-2, SW-2, S-2 E-1, E-2, E-3,	150.9	(495 m, 495 m)	202.42	58.31
3-7	N-2, NW-1, SW-1, S-2,SE-1, NE-1, E-2	123.7	(495 m, 495 m)	199.15	60.73
3-8	N-2, NW-2, SW-2, S-2, E-1, E-2,E-3	157.9	(495 m, 495 m)	202.42	57.43

Note that the pumping source is located at (495 m, 495 m) and the pumping rate and period are respectively 200 CMD and 60 minutes.

Table 7 The identified results with the observations measured at two different time steps

Case	Number of observation wells	Observation wells	Identified results		
			Source location	Pumping rate (CMD)	Pumping period (min)
4-1	4	N-1, W-1, S-1, E-1	(495 m, 495 m)	202.18	57.43
4-2		N-2, W-2, S-2, E-2	(495 m, 495 m)	198.66	61.29
4-3		NW-2, SW-2, E-3, E-1	(495 m, 495 m)	198.38	60.81
4-4	3	W-1, S-1, E-2	(495 m, 495 m)	198.64	61.32
4-5		N-1, W-1, S-1	(495 m, 495 m)	198.62	61.63
4-6		N-1, E-2, S-1	(495 m, 495 m)	198.58	61.58
4-7		N-1, W-1, E-2	(495 m, 495 m)	198.45	61.42
4-8		N-2, S-2, E-2	(495 m, 495 m)	197.88	60.92
4-9		N-2, W-1, S-2	(495 m, 495 m)	198.45	61.35
4-10		W-1, S-2, E-2	(495 m, 495 m)	198.48	61.72
4-11		N-2, W-1, E-2	(495 m, 495 m)	197.85	60.67
4-12	2	W-1, E-2	*(565 m, 385 m)*	*216.79*	*50.48*
4-13		S-1, E-2	(495 m, 495 m)	198.36	60.93
4-14		N-1, E-2	(495 m, 495 m)	197.17	62.04
4-15		W-1, S-1	*(425 m, 415 m)*	*199.51*	*59.87*
4-16		N-1, W-1	(495 m, 495 m)	198.12	61.42
4-17		N-1, S-1	(495 m, 495 m)	199.63	60.59
4-18		N-2, S-2	*(495 m, 475 m)*	*203.43*	*58.46*
4-19		S-2, E-2	(495 m, 495 m)	198.18	61.32
4-20		W-1, S-2	*(565 m, 385 m)*	*216.67*	*50.14*
4-21		N-2, E-2	(495 m, 495 m)	198.42	60.68
4-22		N-2, W-2	(495 m, 495 m)	198.32	61.32
4-23		W-1, E-2	(495 m, 495 m)	197.43	62.43

Note that the pumping source is located at (495 m, 495 m) and the pumping rate and period are respectively 200 CMD and 60 minutes.

Table 8 The location and measured hydraulic head at observation wells for
homogeneous and isotropic unconfined aquifer

Observation well	Location	Measured heads(m)	
		Initial state	T = 8 (hr)
N-1	(465 m, 495 m)	35.393	35.047
N-2	(395 m, 495 m)	35.392	35.388
W-1	(495 m, 425 m)	36.072	36.044
W-2	(495 m, 395 m)	36.359	36.355
S-1	(585 m, 495 m)	35.393	35.384
S-2	(595 m, 495 m)	35.393	35.388
E-1	(495 m, 535 m)	34.999	34.820
E-2	(495 m, 595 m)	34.400	34.395

Table 9 The identified results with the observations without considering measurement
error for homogeneous and isotropic unconfined aquifer

| Case | Observation wells | Identified results | | |
		Source location	Pumping rate (CMD)	Pumping period (hrs)
5-1	N-1, W-1, S-1, E-1, E-2	(495 m, 495 m)	1201.00	7.98
5-2	N-1, N-2, W-2, S-2, E-2	(495 m, 495 m)	1197.46	8.08
5-3	N-1, N-2, W-1, S-2, E-2	(495 m, 495 m)	1201.71	7.96
5-4	N-2, W-2, S-1, E-1, E-2	(495 m, 495 m)	1201.16	7.94

Note that the pumping source is located at (495 m, 495 m) and the pumping rate and period are respectively given as 1200 CMD and 8 hrs.

Table 10 The hypothetic hydraulic conductivities and the measured heads for σ_y is 0.5 m/s

Case	Observation well	Hydraulic conductivity ($\times 10^{-6}$ m/s)	Measured head (m)	
			T =30 min	T = 60 min
6-1	N-1	6.55	22.797	21.565
	W-1	2.74	25.031	24.347
	S-1	4.11	24.639	24.164
	E-1	8.47	23.063	21.984
6-2	N-1	9.49	22.729	21.496
	W-1	2.80	25.084	24.427
	S-1	4.92	24.565	24.036
	E-1	4.79	22.923	21.822
6-3	N-1	3.38	22.828	21.548
	W-1	4.12	25.139	24.500
	S-1	10.41	24.709	24.267
	E-1	4.31	22.777	21.563
6-4	N-1	4.21	22.791	21.831
	W-1	3.03	25.113	24.552
	S-1	9.92	24.727	24.350
	E-1	4.94	23.070	22.178
6-5	N-2	2.68	24.780	24.414
	W-2	7.86	25.732	25.341
	S-2	4.17	24.731	24.332
	E-2	7.11	23.792	23.424
6-6	N-2	2.71	24.751	24.355
	W-2	9.19	25.734	25.341
	S-2	4.78	24.675	24.246
	E-2	5.25	23.778	23.421
6-7	N-2	7.70	24.731	24.326
	W-2	2.79	25.801	25.453
	S-2	3.90	24.792	24.423
	E-2	7.47	23.764	23.367
6-8	N-2	2.64	24.760	24.430
	W-2	8.94	25.790	25.474
	S-2	4.96	24.783	24.467
	E-2	5.34	23.807	23.516
6-9	NW-1	2.50	25.916	25.728
	SW-1	6.44	25.938	25.770
	SE-1	4.94	23.982	23.810
	NE-1	7.87	23.992	23.846
6-10	NW-1	5.00	25.942	25.770
	SW-1	2.47	25.935	25.762
	SE-1	6.81	23.953	23.777
	NE-1	7.43	23.937	23.780
6-11	NW-1	4.80	25.938	25.769
	SW-1	4.13	25.967	25.810
	SE-1	3.13	23.966	23.791
	NE-1	10.08	23.962	23.767
6-12	NW-1	8.22	25.945	25.800
	SW-1	2.67	25.955	25.819
	SE-1	4.26	23.994	23.852
	NE-1	6.68	23.970	23.834

Table 11 The hypothetic hydraulic conductivities and the measured heads for σ_y is 1.0 m/s

Case	Observation well	Hydraulic conductivity ($\times 10^{-6}$ m/s)	Measured head (m)	
			T = 30 min	T = 60 min
7-1	N-1	9.19	22.664	21.277
	W-1	1.70	24.993	24.231
	S-1	2.78	24.675	24.204
	E-1	14.40	23.242	22.089
7-2	N-1	13.30	23.180	21.875
	W-1	1.34	25.064	24.287
	S-1	4.13	24.697	24.204
	E-1	8.47	23.178	22.042
7-3	N-1	10.40	22.746	21.209
	W-1	1.22	25.024	24.259
	S-1	9.97	24.857	24.484
	E-1	4.94	22.764	21.400
7-4	N-1	14.90	21.975	20.424
	W-1	1.79	25.146	24.472
	S-1	2.62	24.803	24.405
	E-1	8.94	22.733	21.393
7-5	N-2	14.10	24.781	24.368
	W-2	6.25	25.810	25.457
	S-2	1.28	24.723	24.298
	E-2	5.56	23.847	23.558
7-6	N-2	1.32	24.831	24.501
	W-2	13.00	25.595	25.072
	S-2	4.26	24.762	24.343
	E-2	8.55	23.776	23.382
7-7	N-2	1.43	24.882	24.607
	W-2	16.50	25.776	25.383
	S-2	4.87	24.912	24.592
	E-2	5.44	23.765	23.331
7-8	N-2	1.19	24.665	24.129
	W-2	10.80	25.779	25.400
	S-2	5.43	24.836	24.487
	E-2	8.95	23.821	23.481
7-9	NW-1	9.02	25.981	25.826
	SW-1	1.62	25.992	25.855
	SE-1	2.98	23.985	23.818
	NE-1	14.36	24.045	23.923
7-10	NW-1	2.50	26.004	25.869
	SW-1	2.45	25.982	25.858
	SE-1	4.94	23.943	23.796
	NE-1	20.64	24.024	23.915
7-11	NW-1	8.22	25.986	25.865
	SW-1	1.14	25.964	25.825
	SE-1	6.64	23.979	23.831
	NE-1	10.04	23.923	23.744
7-12	NW-1	3.15	25.913	25.724
	SW-1	2.54	25.975	25.798
	SE-1	3.54	23.995	23.854
	NE-1	22.09	23.970	23.816

Table 12 The hypothetic hydraulic conductivities and the measured heads for σ_y is 1.5 m/s

Case	Observation well	Hydraulic conductivity ($\times 10^{-6}$ m/s)	Measured head (m)	
			T = 30 min	T = 60 min
8-1	N-1	6.68	22.288	21.166
	W-1	1.53	25.020	24.355
	S-1	1.62	24.603	24.154
	E-1	36.70	23.326	22.422
8-2	N-1	31.60	23.502	22.588
	W-1	1.23	24.769	23.984
	S-1	1.80	24.809	24.446
	E-1	8.94	23.361	22.474
8-3	N-1	35.10	21.220	19.761
	W-1	0.93	25.412	24.961
	S-1	5.34	24.698	24.341
	E-1	3.60	22.705	21.506
8-4	N-1	20.30	23.995	23.097
	W-1	0.63	25.220	24.677
	S-1	9.65	24.451	23.875
	E-1	4.94	22.136	20.693
8-5	N-2	20.80	24.762	24.371
	W-2	1.82	25.702	25.322
	S-2	1.06	24.711	25.328
	E-2	15.58	23.864	23.618
8-6	N-2	0.62	24.727	24.374
	W-2	20.80	25.652	25.235
	S-2	5.43	24.887	24.569
	E-2	8.96	23.888	23.591
8-7	N-2	0.77	24.868	24.591
	W-2	27.20	26.027	25.880
	S-2	3.60	24.765	24.449
	E-2	8.32	23.844	23.458
8-8	N-2	0.77	24.877	24.661
	W-2	30.50	25.843	25.565
	S-2	4.95	24.540	24.026
	E-2	5.34	23.807	23.431
8-9	NW-1	1.31	25.940	25.786
	SW-1	5.43	25.970	25.833
	SE-1	2.22	23.992	23.857
	NE-1	39.65	24.032	23.945
8-10	NW-1	3.15	25.993	25.911
	SW-1	1.31	25.894	25.734
	SE-1	3.53	23.974	23.868
	NE-1	42.91	24.007	23.913
8-11	NW-1	2.76	26.063	26.025
	SW-1	1.74	25.975	25.861
	SE-1	2.81	23.953	23.836
	NE-1	46.28	24.020	23.891
8-12	NW-1	8.22	25.990	25.889
	SW-1	0.59	25.925	25.761
	SE-1	6.67	23.888	23.729
	NE-1	19.40	24.046	23.937

Table 13 The identified results while the conductivity field is perfectly known

| Case | Identified results | | |
	Source location	Pumping rate (CMD)	Pumping period (min)
$\sigma_y = 0.5$ m/s			
6-1	(495 m, 495 m)	199.73	60.12
6-2	(495 m, 495 m)	199.69	60.14
6-3	(495 m, 495 m)	200.12	59.81
6-4	(495 m, 495 m)	199.34	60.20
6-5	(495 m, 495 m)	200.06	59.93
6-6	(495 m, 495 m)	200.28	59.12
6-7	(495 m, 495 m)	199.64	60.28
6-8	(495 m, 495 m)	199.86	60.08
6-9	(495 m, 495 m)	199.64	60.14
6-10	(495 m, 495 m)	200.14	59.93
6-11	(495 m, 495 m)	199.75	60.12
6-12	(495 m, 495 m)	200.22	59.88
$\sigma_y = 1.0$ m/s			
7-1	(495 m, 495 m)	200.20	59.90
7-2	(495 m, 495 m)	199.55	60.24
7-3	(495 m, 495 m)	199.79	60.11
7-4	(495 m, 495 m)	200.38	59.83
7-5	(495 m, 495 m)	199.50	60.25
7-6	(495 m, 495 m)	200.26	59.90
7-7	(495 m, 495 m)	200.18	59.03
7-8	(495 m, 495 m)	199.40	60.34
7-9	(495 m, 495 m)	199.49	60.28
7-10	(495 m, 495 m)	199.71	60.12
7-11	(495 m, 495 m)	199.98	60.00
7-12	(495 m, 495 m)	200.03	59.97
$\sigma_y = 1.5$ m/s			
8-1	(495 m, 495 m)	199.85	60.07
8-2	(495 m, 495 m)	200.25	59.11
8-3	(495 m, 495 m)	199.75	60.07
8-4	(495 m, 495 m)	199.75	60.09
8-5	(495 m, 495 m)	200.26	59.90
8-6	(495 m, 495 m)	200.15	59.97
8-7	(495 m, 495 m)	200.08	60.00
8-8	(495 m, 495 m)	199.67	60.12
8-9	(495 m, 495 m)	199.61	60.15
8-10	(495 m, 495 m)	199.68	60.11
8-11	(495 m, 495 m)	199.68	60.11
8-12	(495 m, 495 m)	200.11	59.95

Note that the pumping source is located at (495 m, 495 m) and the pumping rate and period are respectively 200 CMD and 60 minutes.

Table 14 The examination of the identified results on the monitoring well distribution with the σ_y is 0.5 m/s and conductivity field is perfectly known

Case	Observation wells	Identified results		
		Source location	Pumping rate (CMD)	Pumping period (min)
9-1	SE-1, NE-1, E-2	(495 m, 495 m)	199.71	60.14
9-2	S-2, SE-1, E-2	(495 m, 495 m)	199.72	60.15
9-3	SE-1, E-2, E-3	(495 m, 495 m)	200.26	59.89
9-4	SE-1, E-3 ,NE-1	(495 m, 495 m)	199.63	60.20
9-5	NW-1, W-2, SW-1	(495 m, 495 m)	200.23	59.95
9-6	N-2, NW-2, W-2	(495 m, 495 m)	199.71	60.11
9-7	NW-1, W-1, SW-1	(495 m, 495 m)	200.30	59.91

Note that the pumping source is located at (495 m, 495 m) and the pumping rate and period are respectively 200 CMD and 60 minutes.

Table 15 The hydraulic conductivity for generating the random conductivity field and
the corresponding measured heads

Scenario	σ_y (m/s)	Observation well	Hydraulic conductivity ($\times 10^{-6}$ m/s)	Measured head (m)	
				T = 30 min	T = 60 min
10	0.5	N-1	5.40	22.847	21.506
		W-1	2.41	25.148	24.499
		S-1	6.79	24.700	24.256
		E-1	7.07	22.751	21.483
11	1.0	N-1	15.70	23.589	22.579
		W-1	1.39	25.330	24.808
		S-1	4.64	24.689	24.247
		E-1	6.18	21.978	20.602
12	1.5	N-1	10.30	23.790	23.017
		W-1	0.59	25.526	25.236
		S-1	5.58	24.790	24.483
		E-1	18.30	22.228	20.996

Table 16 The location and measured drawdown for Yenliao site

Observation well	Location	Drawdowns(m)	
		T = 10 (min)	T = 20 (min)
A	(92.5, 97.5)	0.529	0.774
B	(87.5, 97.5)	0.130	0.250
C	(77.5, 97.5)	0.038	0.101
D	(107.5, 115.0)	0.001	0.005

Table 17 Identified results for the Yenliao site

Case	Observation wells	Identified results		
		Source location	Pumping rate (L/min)	Pumping period (min)
13-1	A, B, C	(97.5 m, 97.5 m)	10.38	19.29
13-2	A, B, C, D	(97.5 m, 97.5 m)	10.73	18.87
13-3	B, C, D	(97.5 m, 97.5 m)	10.34	19.21
13-4	A, B, D	(97.5 m, 97.5 m)	10.30	19.17

Note that the pumping source is located at (97.5 m, 97.5 m) and the pumping rate and period are respectively 10 L/min and 20 minutes.
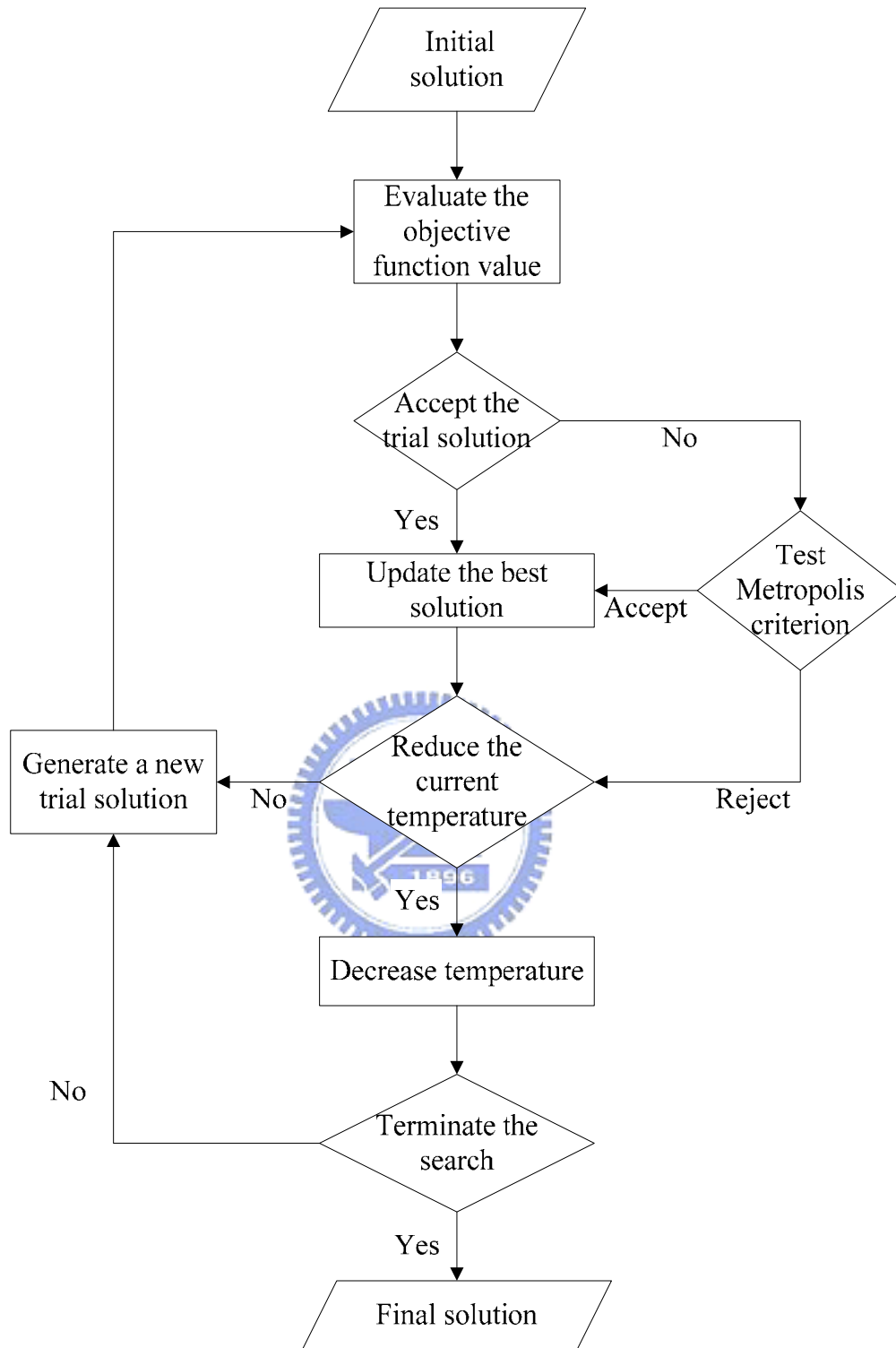
Figure 1 Block flow diagram of SA
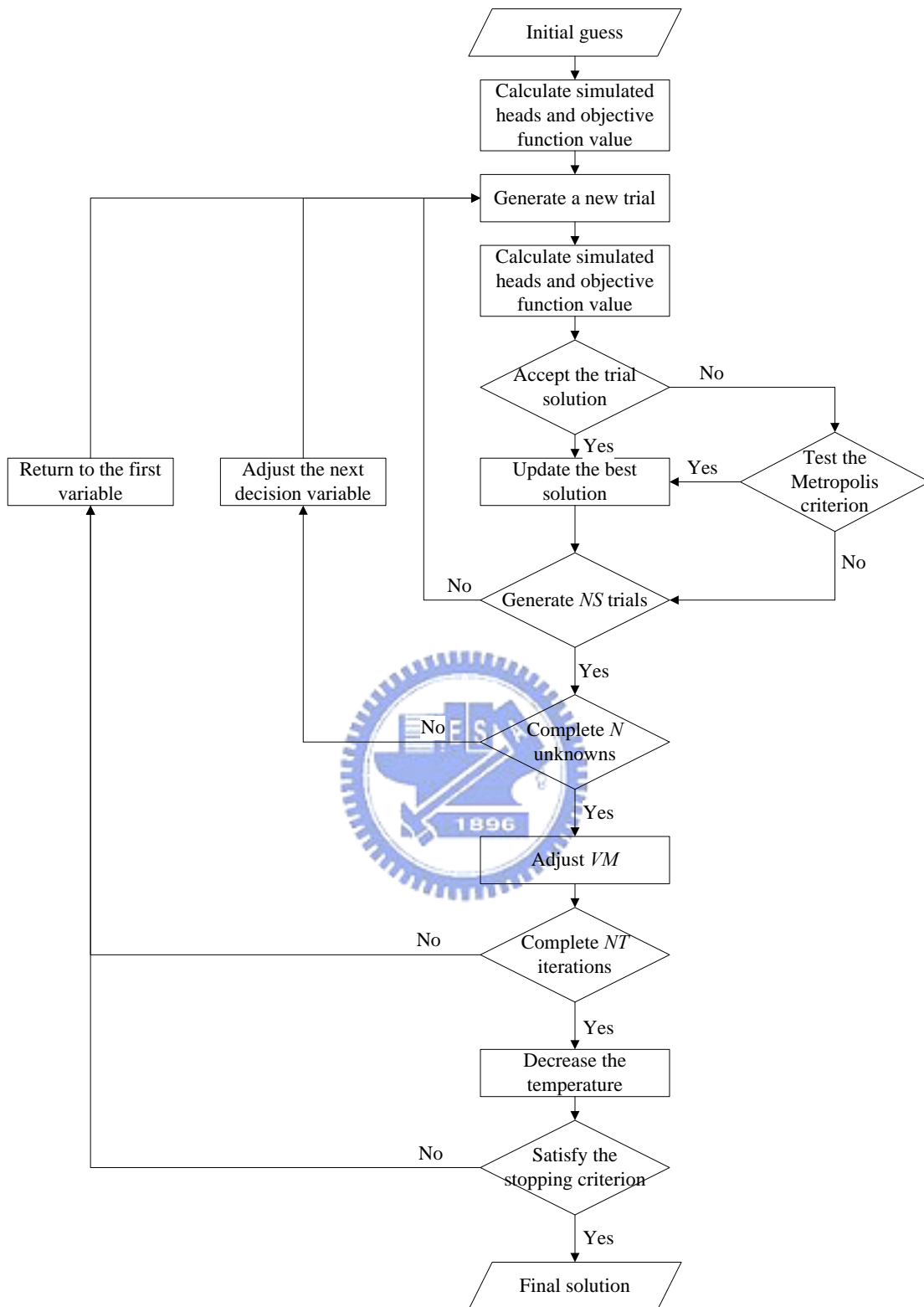
Figure 2 Block flow chart of SA-MF
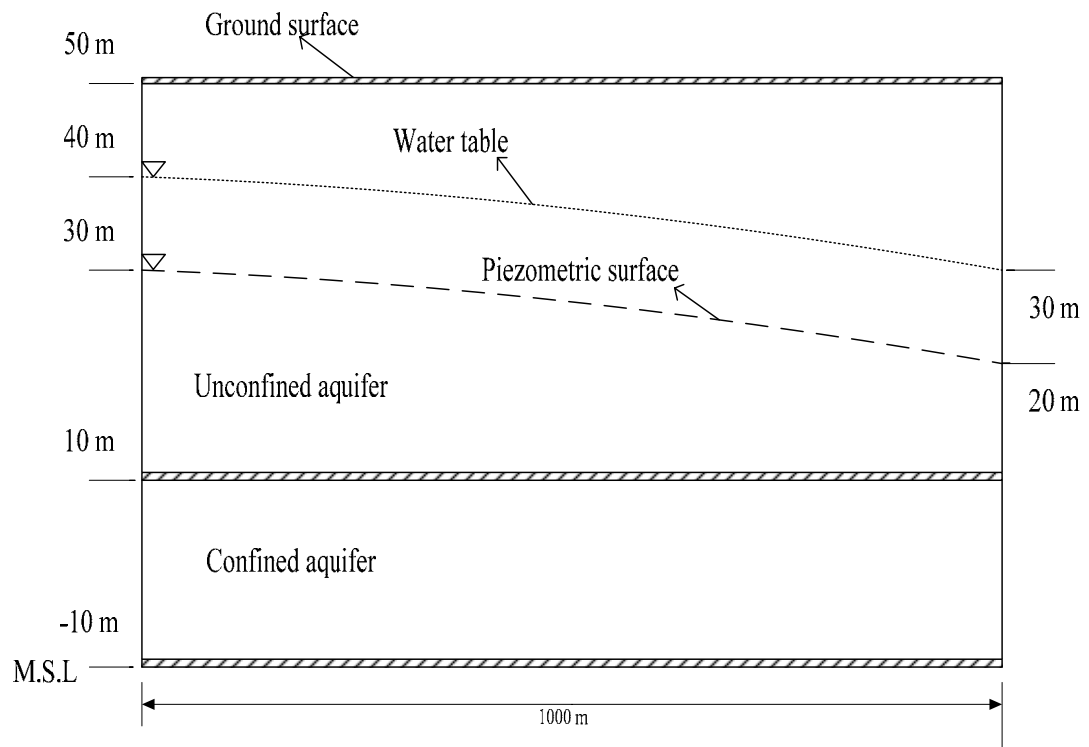
Figure 3 The sectional view of the hypothetic aquifer site
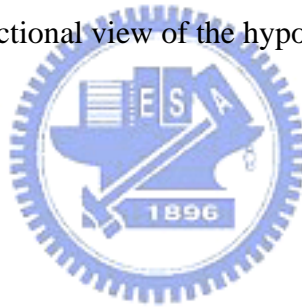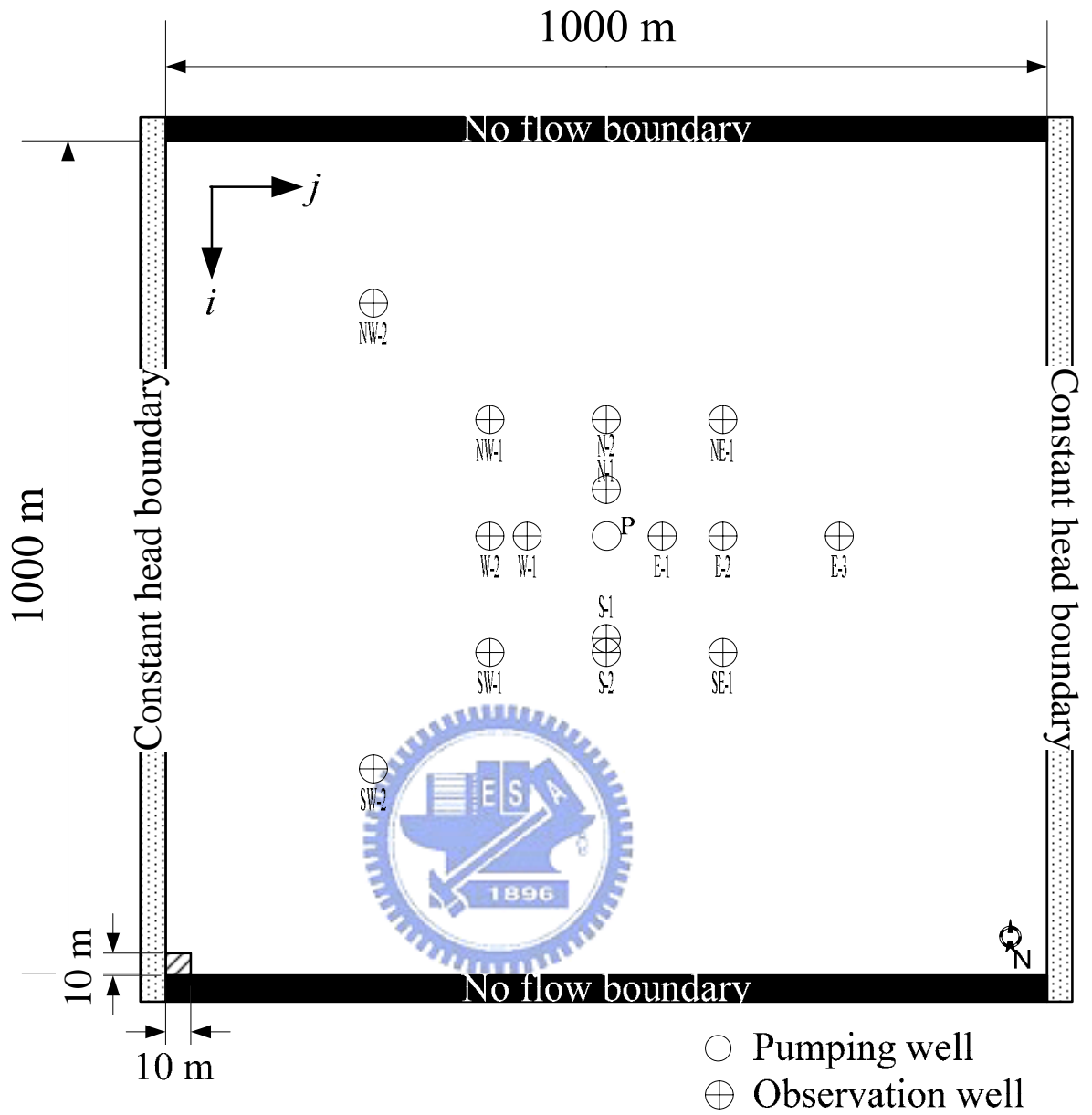
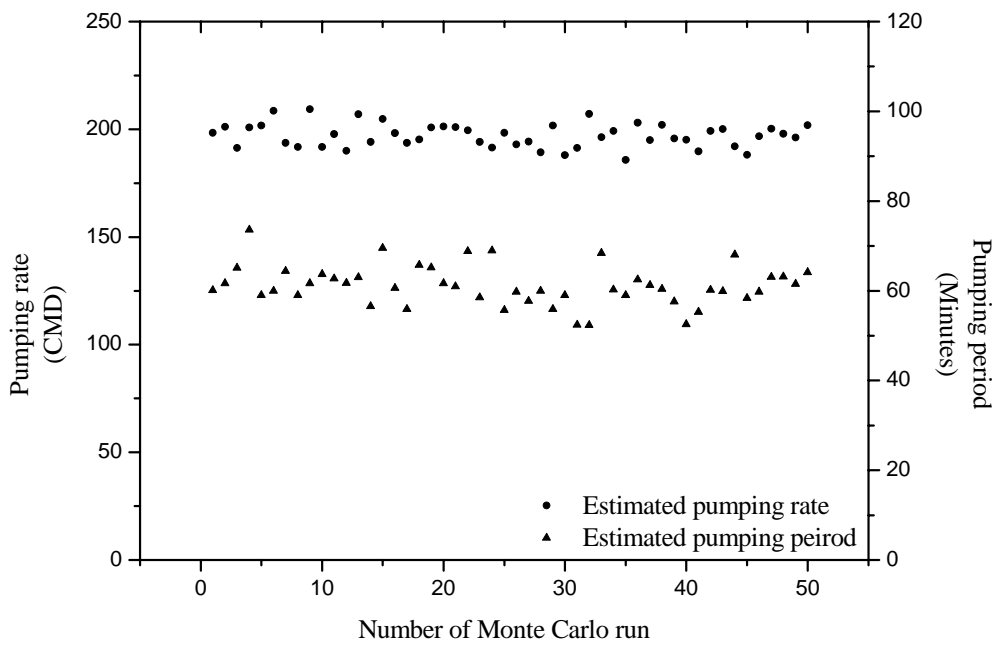Figure 4 The plan view of the hypothetic aquifer site

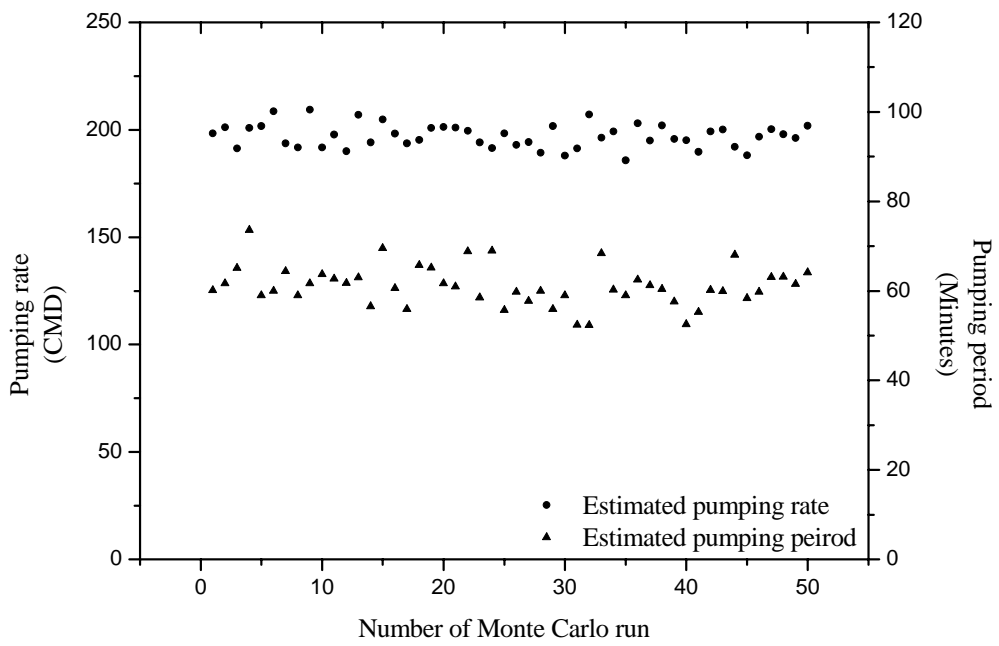Figure 5 Heterogeneous analysis result as σ_y is 0.5 m/s

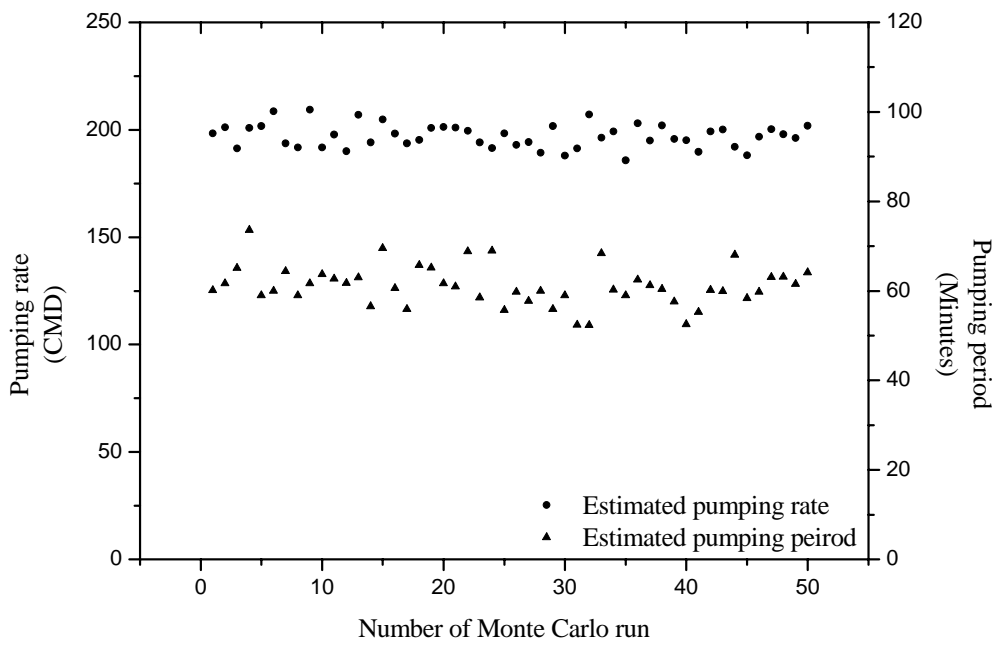Figure 6 Heterogeneous analysis result as σ_y is 1.0 m/s

Figure 7 Heterogeneous analysis result as σ_y is 1.5 m/s
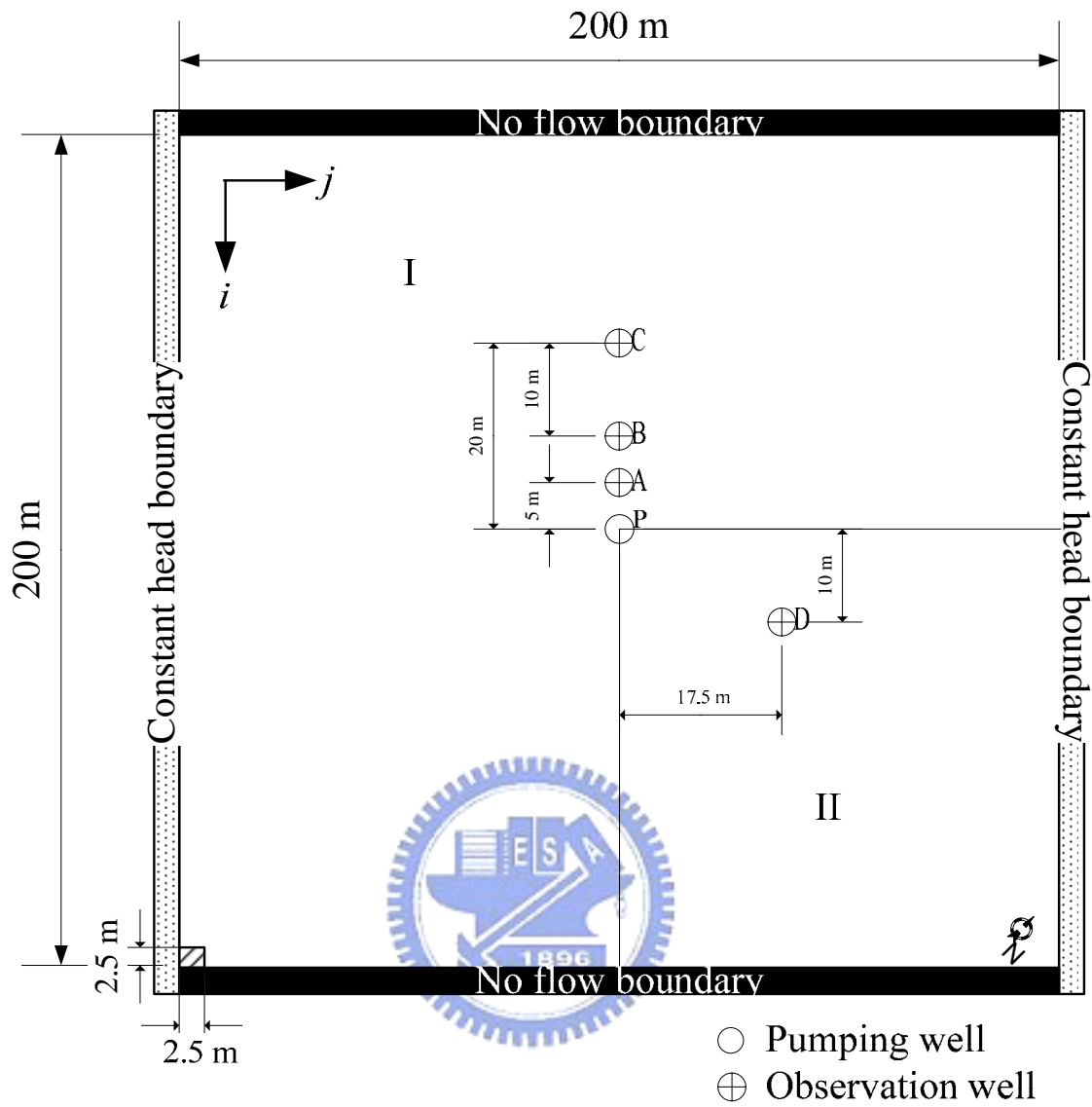
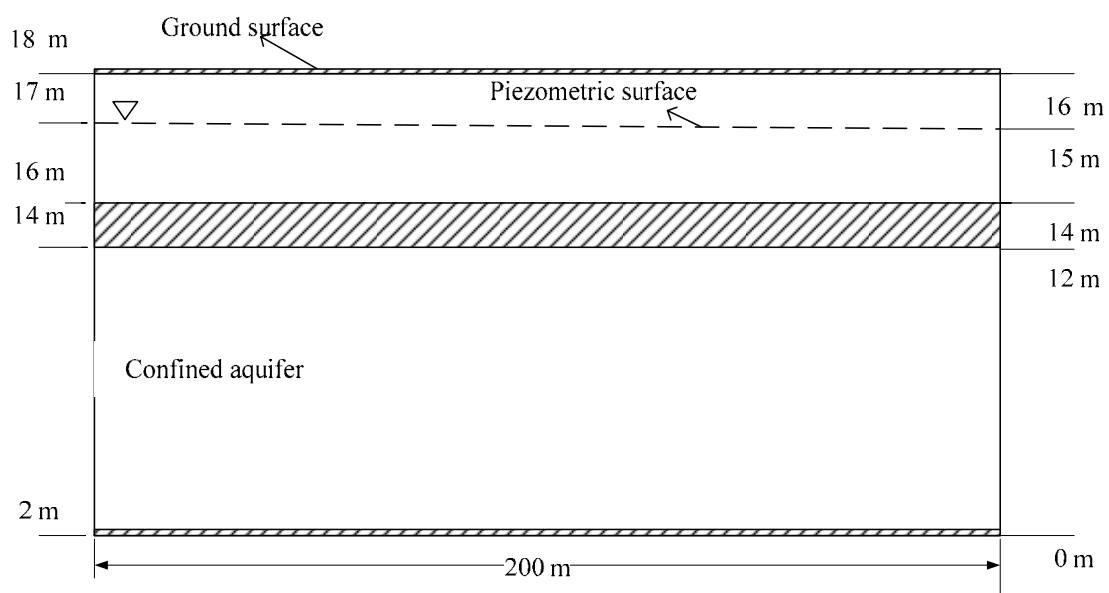Figure 8 The plan view of Yenliao site

Figure 9 The sectional view of Yenliao site

作者簡歷

姓　　名：林郁仲 (Yu-Chung Lin)

出生日期：民國 63 年 6 月 2 日　　　　　　　　出生地：台北市

地　　址：台北市信義區吳興街 269 巷 11 號 4 樓

電　　話：(02)2720-4392

電子郵件：murphy.ev89g@nctu.edu.tw

興　　趣：古典音樂、攝影、登山、旅遊、看電影、閱讀

學　　歷：86.09~89.06　國立台灣大學土木工程學系畢業

　　　　　89.09~91.01　國立交通大學環境工程研究所碩士班

　　　　　91.01~95.02　國立交通大學環境工程研究所博士班

著作目錄

Journal papers

1. <u>Lin, Y.C.</u> and H.D. Yeh (2005), Trihalomethane species forecast using optimization methods: genetic algorithm and simulated annealing, *J. Comp. in Civ. Engrg.*, ASCE, 19(3), 248-257.

2. Yeh, H.D., <u>Y.C. Lin</u>, and Y.C. Huang (2005), Application of simulated annealing and genetic algorithm for identifying leaky aquifer parameters, *Hydrological process*. (Accepted)

3. Yeh, H.D., Y.C. Huang, and <u>Y.C. Lin</u> (2006), A novel approach based on simulated annealing and genetic algorithm to identify the parameters of confined and unconfined aquifers, *Hydrological Sciences Journal*. (in revised)

4. Yeh, H.D. and <u>Y.C. Lin</u> (2006), Pipe network analysis using global optimization method, *Journal of Water Resources Planning and Management*. (revised and in review)

5. Yeh, H.D., T.H. Chang, and <u>Y.C. Lin</u> (2006), Groundwater contaminant source identification by a hybrid heuristic approach, *Water Resour. Res.*. (revised and in review)

6. <u>Lin, Y.C.</u>, and H.D. Yeh (2006), Identifying groundwater contaminant source characteristics using simulated annealing, *Journal of the Chinese Institute of Environmental Engineering*. (in press)

7. Chang, T.H., <u>Y.C. Lin</u>, and H.D. Yeh (2006), Develop a three-dimensional model to determine a constant release contaminant source in groundwater, *Journal of the Chinese Institute of Environmental Engineering*. (in press)

Conference papers

1. <u>林郁仲</u>、葉弘德，90 年 8 月，模擬退火演算法應用於自來水管網系統分析，第八屆全國計算流體力學學術研討會，逢甲大學，宜蘭，G2:1-4 頁。

2. <u>林郁仲</u>、葉弘德，90 年 12 月，模擬退火演算法應用於三鹵甲烷濃度分析，第十四屆環境規劃與管理研討會，高雄第一科技大學，高雄市，論文摘要集 4-65 頁。

3. <u>林郁仲</u>、葉弘德，91 年 11 月，以最佳化方法分析配水管網系統，第十五屆環境規劃與管理研討會，中華民國環境工程學會，台北市，論文集(光碟版)p-e-p01。

4. <u>林郁仲</u>、葉弘德、黃彥禎，92 年 6 月，應用模擬退火演算法於滲漏水層參數之檢定，九十二年電子計算機於土木水利工程應用論文研討會，國立台灣

科技大學，台北市，摘要集 72 頁、論文集(光碟版)數位水利 16。

5. 黃彥禎、葉弘德、<u>林郁仲</u>，92 年 6 月，應用模擬退火演算法於拘限及自由水層參數之檢定，九十二年電子計算機於土木水利工程應用論文研討會，國立台灣科技大學，台北市，摘要集 74 頁、論文集(光碟版)數位水利 18。

6. <u>林郁仲</u>、葉弘德、黃彥禎，92 年 11 月，基因演算法應用於滲漏水層參數檢定，環工學會第十五屆年會及第一屆土壤與地下水技術研討會，國立中興大學，台中，論文集 2-11，論文集(光碟版)B-05。

7. 黃彥禎、葉弘德、徐年盛、<u>林郁仲</u>，92 年 11 月，禁忌演算法於拘限及自由水層參數之檢定，環工學會第十五屆年會及第一屆土壤與地下水技術研討會，國立中興大學，台中，論文集 2-10，論文集(光碟版)B-03。

8. <u>林郁仲</u>、葉弘德、黃彥禎、徐年盛，92 年 12 月，禁忌演算法應用於滲漏含水層參數檢定，第十二屆農工研討會，中國農業工程學會，高雄，論文集 102，論文集（光碟版）995-1006。

9. <u>林郁仲</u>、葉弘德、黃彥禎，滲漏含水層多口觀測井參數檢定，第十四屆水利工程研討會，國立交通大學，新竹市，論文集(下冊)F181-F185 頁。

10. 張君豪、葉弘德、黃彥禎、<u>林郁仲</u>，93 年 7 月，以模擬退火演算法方法推求定流量試驗受壓含水層之雙層參數，第十四屆水利工程研討會，國立交通大學，新竹市，論文集(下冊)F30-F36 頁。

11. 張桐樺、<u>林郁仲</u>、葉弘德，93 年 7 月，以模擬退火演算法方法推求地下水污染源，第十四屆水利工程研討會，國立交通大學，新竹市，論文集(下冊)F23-F29 頁。

12. 黃彥禎、葉弘德、<u>林郁仲</u>，93 年 7 月，滲漏含水層參數即時檢定模式之比較，第十四屆水利工程研討會，國立交通大學，新竹市，論文集(下冊)F186-F192 頁。.

13. <u>林郁仲</u>、葉弘德，93 年 10 月，以二維解析解推求地下水污染源，九十三年度農業工程研討會，中國農業工程學會，桃園，論文摘要集 246 頁，論文集光碟版 1530-1537 頁。

14. <u>Lin, Y.C.</u> and H.D. Yeh (2004), Uncertainty Analysis in Identifying the Source Location and Release History, Eos Trans. AGU, 85(47), Fall Meet. Suppl., Abstract H13B-0408.

15. 陳淇汾、<u>林郁仲</u>、與葉弘德，重建地下水污染歷程：模擬退火演算法，94 年 6 月，第九屆土壤及地下水污染整治研討會，台灣土壤及地下水環境保護協會，台北，論文集 193-202 頁

16. 張桐樺、<u>林郁仲</u>、與葉弘德，結合禁忌演算法與模擬退火演算法推求地下水污染源，94 年 6 月，第九屆土壤及地下水污染整治研討會，台灣土壤及地下水環境保護協會，台北，論文集 287-300 頁

17. 葉弘德、張桐樺、與<u>林郁仲</u>，94 年 10 月，藉由結合禁忌演算法與模擬退火演算法推求地下水污染源，第十四屆農工研討會，中國農業工程學會，苗栗，

論文集 109。

18. 葉弘德、張桐樺、<u>林郁仲</u>，結合啟發式搜尋法推求地下水污染源，94 年 11
月，第三屆土壤與地下水研討會，環境工程學會，桃園，論文摘要集 505
頁。